

Aalborg University
School of Engineering and Science
Department of Civil Engineering

Title:

Numerical Simulation of Gyroscopic Effects in Ansys

Theme:

Design and analysis of advanced/special structures

Master's Thesis:

07.02.2011 – 19.08.2011

Author:

Christian Jensen

Supervisors:

Lars Damkilde

Ronnie Refstrup Pedersen

Number of printed:

4

Number of pages:

78

CD enclosed:

1

Preface

This master thesis has been made in the period 7th of February 2011 to 19th of August 2011 at the 10th semester at the Department of Civil Engineering at Aalborg University Esbjerg. The project has been initiated by Rambøll Oil & Gas and I would in that context express my gratitude to Ulf Tygesen and Thomas Larsen.

Furthermore, I express my gratitude to my supervisors Professor Lars Damkilde and Associate Professor Ronnie R. Pedersen for their support and supervision during this thesis work.

This research is financially supported by grants from SUC Fund Esbjerg # 2010-5745.

Finite Element Analysis is performed in Ansys Classic Version 12 and the results are post-processed in Matlab. Commands in Ansys are mentioned as ‘CORIOLIS,on,,,on’.

References are mentioned by chapter number, X, and a number, Y, [X,Y] referring to the bibliography in the end of each chapter. Figures without reference are own material.

A CD with lgw-files for the Finite Element analysis, Matlab files (M-files) and this thesis in pdf-format is enclosed.

Aalborg University Esbjerg, August 2011.

Christian Jensen

Abstract

The subject of this thesis is Numerical Simulation of Gyroscopic Effects in Ansys. A natural frequency analysis and a transient response analysis are performed in Ansys Classic for a simple rotor configuration. The results are verified with analytical solutions.

The structural response of a floating wind turbine is analyzed and the influence of gyroscopic effects is examined. This is done by comparing two situations where in the first situation the wind turbine is analyzed in parked condition and in the second situation in operational mode.

The gyroscopic effect introduces additional forces and vibrations in the tower of the wind turbine. However, these forces are very small compared to forces generated by the wave motion of the wind turbine. The tendencies observed in this thesis work correspond to previous research.

Synopsis

Rapporten omhandler numerisk simulation af gyroskopiske effekter i Ansys Classic. En egenfrekvens analyse og en transient respons analyse udføres i Ansys for en simpel rotor konfiguration. Resultaterne er verificeret med analytiske beregninger.

Det strukturelle respons er analyseret for en flyende vindmølle og den gyroskopiske effekt er undersøgt. Dette er gjort ved at sammenligne to situationer, hvor vindmøllen i den første situation er analyseret i parkeret tilstand og i den anden situation i operationel tilstand.

Den gyroskopiske effekt genererer ekstra kræfter og vibrationer i vindmølletårnet. Disse kræfter er i midlertidig meget små i forhold til de kræfter, der genereres som følge af bølgebevægelsen af vindmøllen. De observerede tendenser i dette projekt svarer overens med tidligere forskning.

Table of contents

Abstract.....	V
Synopsis.....	VII
Table of contents	X
1 Introduction.....	1
1.1 Definition and Properties of a Gyroscopes.....	1
1.2 Gyroscopic forces in Structural Engineering –Wind Turbines	5
1.3 Objective.....	8
1.4 Outline	9
1.5 References	9
2 Basic Rotor Dynamics	11
2.1 Preliminaries.....	11
2.2 A simple rotor model – Governing equations	15
2.3 Summery	20
2.4 References	20
3 Ansys – Preprocessor.....	21
3.1 Presenting the Reference Model	21
3.2 Building the Model - Preprocessor	22
3.3 Summery	24
3.4 References	24
4 Natural frequency Analysis	25
4.1 Natural Frequency Analysis in Ansys	25
4.2 Natural Frequency Analysis - Analytical Solution.....	26
4.3 Comparison – Numerical and Analytical Solution.....	27
4.4 Parameter Study of an Overhang Rotor	28
4.5 Summary	33
4.6 References	33
5 Transient Analysis	35
5.1 Defining the Motion.....	35
5.2 Transient Analysis in Ansys	35
5.3 Summary	38
5.4 References	38
6 Analysis of a Floating Wind Turbine.....	39
6.1 Generation of the Wind Turbine Model.....	39
6.2 Natural Frequency Analysis	42
6.3 Transient Analysis of the Wind Turbine.....	43
6.4 Results of the Transient Analysis.....	47
6.5 Summary	54
6.6 Discussion of the Results and Methods.....	55
6.7 References	56

7	Conclusion	57
8	Overview of the Attached Disk.....	58
8.1	Anslys LGW files	58
8.2	Matlab Plotting Routines.....	59
	Appendix A	60
	A.1 Derivation of the Stiffness Matrix	60
	Appendix B	61
	B.1 Stationary vs. Rotating Reference Frame	61
	Appendix C	62
	C.1 Natural Frequencies for the Simple Rotor Configuration	62
	Appendix D	65
	D.1 Modeling of Bearings	65
	Appendix E	67
	E.1 Analysis of the Support Springs.....	67
	Appendix F.....	70
	F.1 Solving the Equation of Motion for a Simple System.....	70
	F.2 Solving the Equation of Motion in Maple	71
	Appendix G – Results Chapter 7	72
	G.1 Displacement in the x-Direction for Model 1 and Model 2	72
	G.2 Rotations about the z-axis for Model 1 and Model 2	72
	G.3 Rotation about the y-axis Model 2.....	72
	Appendix H.....	74
	H.1 Unbalance load	74
	H.2 Harmonic Analysis in Ansys	74
	H.3 Analytical Solution.....	75
	H.4 Comparison – Numerical and Analytical Solution	76

1 Introduction

This report focuses on the modeling of gyroscopic effects. Gyroscopic effects are present in the daily life and often without noticing it. As an example, the gyroscopic effect makes it possible to walk with a bicycle while only holding it onto the saddle and then steering it to the side by quickly tilting the bicycle. In principle the gyroscopic effect works like this: If we have a wheel that spins about its spin axis and is tilted about a second axis the wheel will try to rotate about the third axis due to the gyroscopic effect. In this report we examine how to include gyroscopic effects in the Finite Element Method (FEM) program Ansys and apply this modeling technique to real life structures and examine how gyroscopic effects affect the dynamic response and natural frequencies.

Next, we will introduce the gyroscopic effect by considering a simple gyroscope and take a look at different mechanical- and structural systems affected by gyroscopic effects.

1.1 Definition and Properties of a Gyroscopes

A gyroscope is a spinning disk where rotation about the x , y and z axis is possible. In practice, this is achieved when a rotating axle is mounted into two frames, as shown in Figure 1.1, which allows the rotating axle AB to take any position in space. This kind of gyroscope has three degrees of freedom; rotation about the axes AB, DE, and GK. All Axes intersect in the center of suspension O.

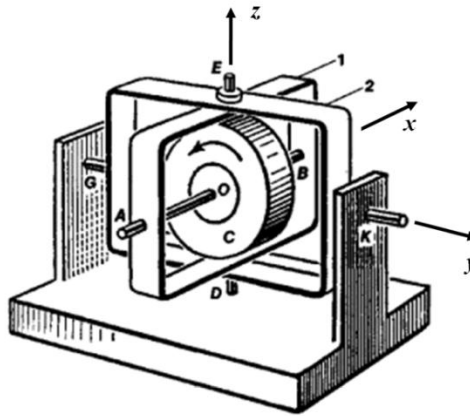


Figure 1.1 Gyroscope in a gimbal suspension mounted in the frames 1 and 2. The disk C is rotating about its axis AB but can also rotate together with frame 1 about the axis DE and, together with frame 2, about the axis GK [0.1].

The spinning disk has an angular momentum L_x given by $I_p \Omega$, where I_p is the polar mass moment of inertia and Ω is the angular velocity of the gyroscope's own rotation about the x -axis. We know from classic mechanics [0.2] that the angular momentum is constant for a closed system, also known as the principle of conservation of angular momentum. This quantity is essential in the analysis of gyroscopes and results in two important properties of a gyroscope. Firstly, a spinning gyroscope will resist changes in the orientation of its spin axis. Second, if a twisting

force is applied to the spin axis, the axis does not turn in the direction of the twisting force, as would be the case with an axle in rest, but instead the axle moves in a direction perpendicular to the both the applied twisting force and the angular momentum. This motion is called precession. The precession motion can be explained by the gyroscope illustrated in Figure 1.2.

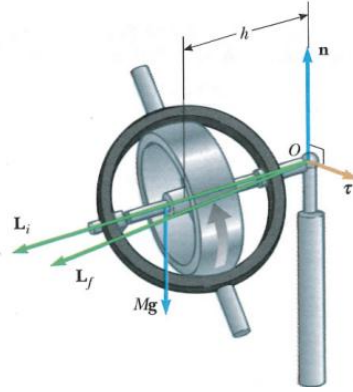


Figure 1.2 Motion of a gyroscope. The gravitational force Mg produces a torque about the pivot. The torque is perpendicular to the axle, [0.2].

1.1.1 Governing Equations for a Gyroscope

The spin axis of the gyroscope is, as shown in Figure 1.2, placed in the horizontal plane and loosely supported from one end. The unsupported end of the rotating gyroscope will not fall, as one might expect, but instead start to move in circular path about the vertical axis. There is a normal force n acting upwards at the pivot and a downward gravitational force Mg . The gravitational force produces a torque $\tau = Mgh$ about O . There is a relation between the torque τ and the angular momentum L defined by [0.2]

$$\tau = \frac{dL}{dt}, \quad (1.1)$$

which is the rotational analog of Newton's second law, $F = \frac{dP}{dt}$, where P is the linear momentum defined by $P = mv$, where m is the mass and v is the velocity of the mass. Equation (1.1) states that the torque acting is equal to the time rate change of the particles angular momentum [0.2]. The torque τ produces a change in angular momentum dL , which are in the same direction as τ and perpendicular to L . In summery; the gyroscope spins about one axis, the gravitational force creates a torque about a second axis. As a result, the gyroscope rotates about the third axis. The motion about the third axis is called the precession motion. The effect which causes this motion is called a gyroscopic effect.

This report focuses on the modeling of this effect. One could expect that this effect comes out naturally in a commercial Finite Element Analysis (FEM) programs like Ansys but this is not the case. However, it is possible to include a gyroscopic effect in an analysis but this requires certain commands to be activated. It is important to include the gyroscopic effect in the analysis of

structural and mechanical systems which behave like a gyroscope. Since the gyroscopic effect can influence both the natural frequencies and adds additional forces into a system.

The angular velocity of the procession motion can be calculated from the vector diagram, shown in Figure 1.3.

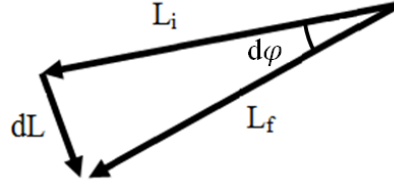


Figure 1.3 Overhead view. The torque τ result in a change in angular momentum dL . The axle sweeps out an angle $d\theta$ in the time interval dt . The magnitude of L does not change, i.e. $L_{initial} = L_{final}$.

From the vector diagram we see that

$$\sin(d\theta) \approx d\theta = \frac{dL}{L} = \frac{\tau dt}{L} = \frac{(Mgh)dt}{L}, \quad (1.2)$$

and with the assumptions of small rotations $\sin(\theta) \approx \theta$ and dividing by dt and $dt \rightarrow 0$ we find

$$\omega_p = \frac{d\theta}{dt} = \frac{Mgh}{L}. \quad (1.3)$$

Equation (1.3) describes the relation between the torque τ (Mgh), the angular momentum L , and the procession motion velocity ω_p . ω_p is increasing when the angular momentum L , defined by $I_p\Omega$, is decreasing. Equation (1.3) is only valid if $\Omega \gg \omega_p$. Equation (1.3) is useful in the analysis of structural systems affected by gyroscopic effects. This is demonstrated in the following section.

1.1.2 Simple Rotor Configuration Affected by Gyroscopic Forces

Let us consider a rotor configuration, as shown in Figure 1.4, which consists of a single rigid disk centrally mounted on a uniform flexible massless shaft, supported by two identical rigid bearings at each side.

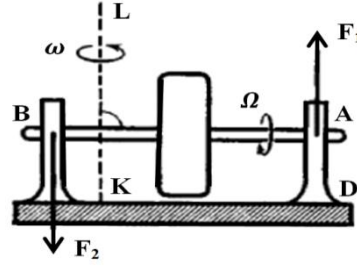


Figure 1.4 The rotor AB is spinning with an angular velocity Ω and undergoes at the same time a rotation ω about the KL axis, [0.1].

The shaft AB, shown in Figure 1.4, rotates with an constant angular velocity Ω and the base rotates about the axis KL with an angular velocity ω . Changing the direction of the angular momentum $I_p\Omega$ result in a toque given by

$$\tau = I_p\Omega\omega. \quad (1.4)$$

Equation (1.4) is obtained by rewriting equation (1.3). The torque is resisted by the support bearings A and B, i.e. the torque results in a two reaction forces, as shown in Figure 1.4, with opposite directions F_1 and F_2 . These forces are called gyroscopic forces. Gyroscopic forces play an important role in the analysis of rotating machinery because they add additional forces into a system. These forces are not included automatically in a FEM analysis and have to be taken into account. In particular the gyroscopic forces are significant if the angular momentum (about the spin axis) is large and the structure/machinery is undergoing a rotation, as shown in Figure 1.5, about the primary- or secondary axis.

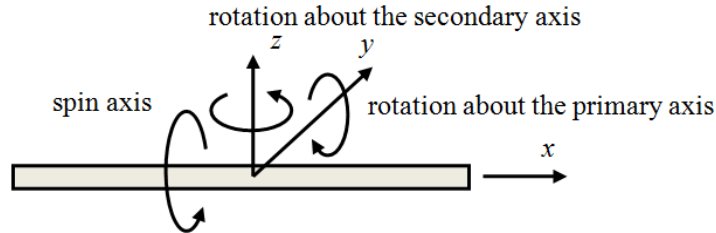


Figure 1.5 Rotor configuration nomenclature.

Ships, aircrafts and wind turbines and many other machineries contain rotating parts; the ships screws, the aircrafts airscrew, the rotor of a wind turbine. Turning the ship, pitching the aircraft, pitching or yawing a wind turbine introduces gyroscopic forces which must be considered in the analysis of these structures. The following section provides some examples of mechanical systems affected by gyroscopic forces.

1.1.3 Example – the Principle of a Car Affected by Gyroscopic Forces

The engine of an automobile motor behaves in the same manner as a gyroscope. When spinning the engine/gyroscope in clockwise direction, seen from the back as shown in Figure 1.6, and

turning the car to the right (clockwise from above) result in a gyroscopic moment forcing the front of the car downwards and the rear end upwards. This is illustrated in Figure 1.6.

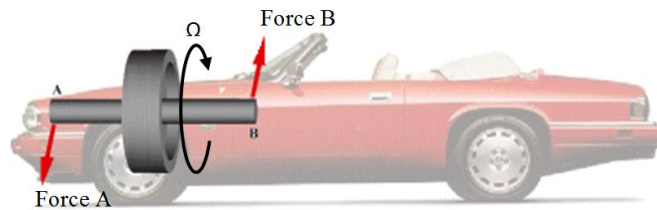


Figure 1.6 Forces on an automobile due to the gyroscopic moment that are created when the engine rotates clockwise (seen from behind) and turning right (clockwise from above), [0.3].

The opposite behavior is observed if the car turns left instead of right. This would lift the front of the car and push bottom down. Spinning the engine in the opposite direction implies a reverse situation. Moving the car pure translational upwards, downwards, forwards, back-wards or side-to-side does not create any gyroscopic forces.

1.1.4 Example – the Principle of an Airplane Affected by Gyroscopic Forces

An airplane can change its pitch altitude by raising or lowering the tail. This is done during take-off or landing. Changing the pitch altitude introduces gyroscopic forces that result, as shown in Figure 1.7, in a yawing motion. Yawing the airplane around the vertical axis results in pitching moment.

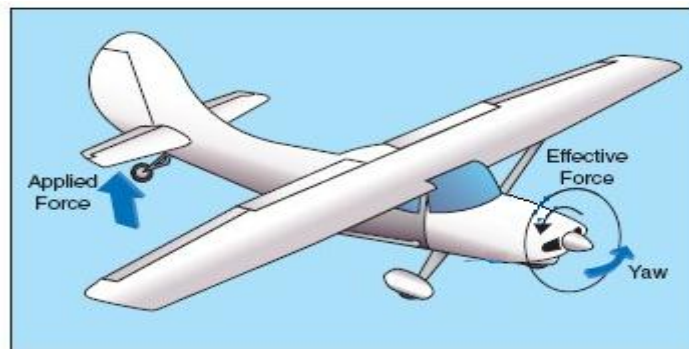


Figure 1.7 Raising the tail of the airplane produces a force that yaw the airplane, [0.4].

1.2 Gyroscopic forces in Structural Engineering –Wind Turbines

Wind turbines, offshore wind turbines and in particular floating offshore wind turbines are structures/machinery that, under the right circumstances, are affected by gyroscopic forces. These forces are caused by the spinning rotor (hub + blades) inertia combined with nodding motion (combination of tower deflection and support platform motion). Figure 1.8 shows the nomenclature. Some literature uses the word “pitch” instead of “nod”.

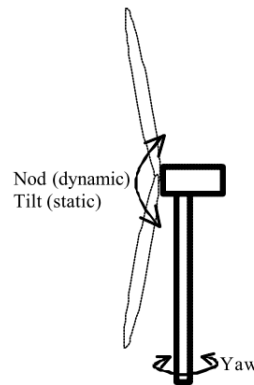


Figure 1.8: Wind turbine nomenclature.

In principle, a wind turbine can move in two motions that generates the gyroscopic forces. These motions are explained in the following section.

1.2.1 Gyroscopic Forces Introduced by Specific Motions of a Wind Turbine

Gyroscopic forces are generated if the rotating rotor is yawed into the wind. The axis of rotation changes in the horizontal plane when the wind turbine is yawing. This introduces a gyroscopic torque perpendicular to the spinning axis and the yawing axis (about the y -axis), as illustrated in Figure 1.9 (a). Modern wind turbines are installed with an active yaw control system which controls the yawing rates. Usually, the yawing rate is so slow (less than 1 deg/s) that forces introduced by the gyroscopic effect do not play an important role, as shown by Lucy Y. Pao et.al [0.5]. A gyroscopic effect can also occur when the tower moves in a nodding motion. Consequently, the rotating rotor then tilts upwards and downwards (following the motion of the tower). This is illustrated in Figure 1.9 (b).

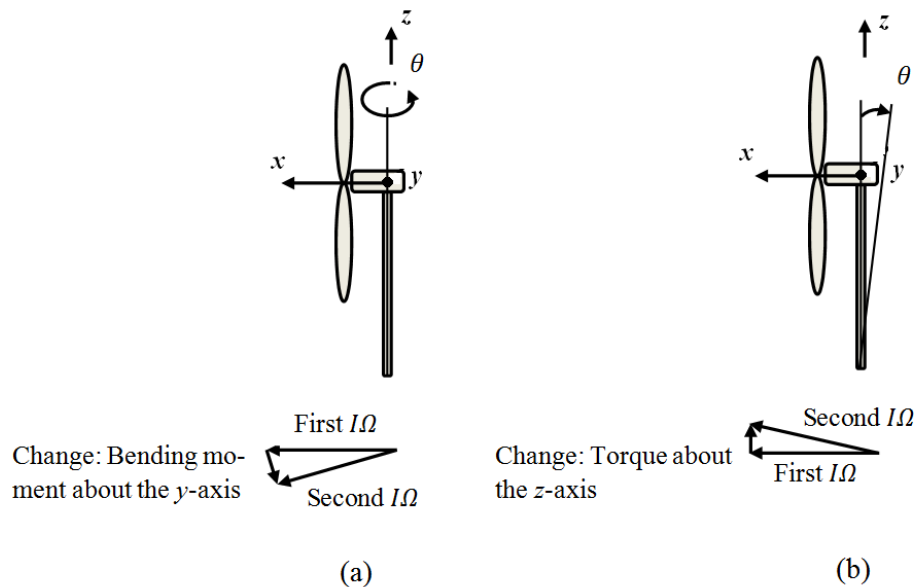


Figure 1.9 (a) The rotating rotor is yawed into the wind. An additional bending moment about the y -axis is introduced due to the gyroscopic effect. (b) The rotating rotor tilts upwards. As a result, a moment is introduced about the z -axis.

1.2.2 Floating Wind Turbines – Additional Gyroscopic Loading

A.R. Henderson et al [0.6] analyzed the motions of a floating wind turbine and concluded that the waves and sea current adds additional motion of all degrees of freedom of the wind turbine except the yaw motion. Typically, yaw motions are not introduced because of symmetry of the floating support structure. However, the nodding motion of the floating wind turbine introduces a torque in the tower of the wind turbine. This means that the yaw response is nonzero even though the yaw motion is not excited by the aerodynamics- or hydrodynamic loads.

1.2.3 Floating Wind Turbines – Previous Research

The increased motions of the support platform adds additional loading to floating wind turbine. Henderson and Patel [0.7] analyzed a 700-kW wind turbine on a floating platform and showed that tower and nacelle loads were heavily affected by inertia loads due to nodding motion of the wind turbine. They conclude that the strength of the tower has to be increased if the platform motions cannot be reduced. Dominique et. al [0.8] draws the same conclusion “The wind turbine may not be able to withstand some of the floater introduced motions”.

J.M.Jonkman et. al [0.9] analyzed an offshore wind turbine supported by a barge with catenary moorings, as shown in Figure 1.10 (right). They used a fully coupled Aero-Hydro-Servo-elastic simulation tool which includes combined wind and wave loading, i.e. the dynamic coupling between the turbine and floating barge were modeled. The main purpose of their work was to compare the loads between an onshore and an offshore wind turbine. They analyzed four different extreme load cases, with similar wind loads for the offshore- and the onshore wind turbine, and took an average value of the extreme values from the sea-based analysis and divided them with the corresponding land-based analysis. Chosen results are presented in Figure 1.10 (left). The dashed horizontal line illustrates a ratio of unity. A ratio larger than one indicates that the offshore wind turbine is affected by the coupling between the turbine and the barge, i.e. the loads increases due to the platform motion.

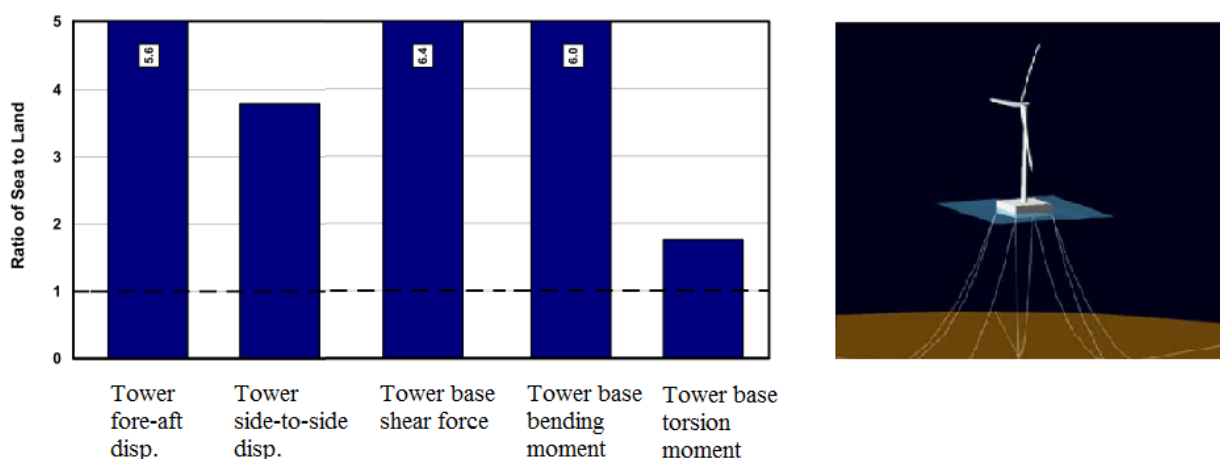


Figure 1.10 Sea- to- land ratios of absolute extreme values from four different load cases. Tower-top fore-aft displacement. Tower side-to-side displacement. Tower base shear force (vector sum of the shear force along the x- and

y-axis). The tower is modeled in the *z*-direction. Tower base bending moment (vector sum of the bending moment about the *x*- and *y*-axis). Tower base torsion moment. Right: offshore wind turbine on a barge [0.9].

It is obvious from Figure 1.10 that a floating offshore wind turbine is much more severely loaded than an identical onshore wind turbine. There are basically two mechanisms that introduce additional loading to the floating wind turbine. The first effect can be explained from, an inverted pendulum, shown in Figure 1.11.

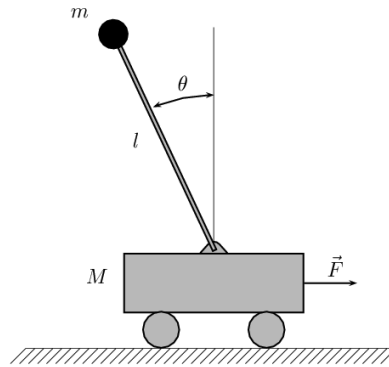


Figure 1.11 Schematic drawing of the inverted pendulum effect [0.10].

The second effect comes from the gyroscopic loading caused by the spinning rotor (hub + blades) inertia combined with a nodding motion (combination of tower deflection and support platform motion). J.M.Jonkman et al find a sea-to land ratio of 5.6 for the tower-top fore-aft displacement and concludes that this is due to the inverse pendulum effect. The large tower side-to-side displacement ratio is due to a yaw motion of the barge which is excited by a gyroscopic yaw moment. This gyroscopic yaw moment is generated from the inertia of the spinning rotor in combination with nodding motion. Tower base shear forces and tower base bending moments are increased due to the inverse pendulum effect. The tower base torsion moment is almost increased with a factor two; this is due to the gyroscopic yaw moment caused by the nodding motion of the spinning rotor.

1.3 Objective

Generally, offshore wind turbines are limited to shallow water depth shallower (< 50 m) where the established monopile foundation, gravity based foundation or jacket technologies can be used. However, in contrast to most of Europe, much of the offshore wind resource potential in Norway, United States, China and Japan is in seas with water depths (> 50 m) [0.9].

The floating wind turbine technology is developing and we want to be able to model the gyroscopic effect in order to examine how this effect affects the dynamic response of a floating wind turbine. Gyroscopic effects are not included automatically in the commercial finite element package Ansys. However, it is possible to activate this effect with special commands.

The primary objective of this thesis work is to analyze a wind turbine supported on a rocking foundation and determine the importance and relevance of gyroscopic effects. The primary objective can only be achieved if we know how to implement the gyroscopic effect in Ansys. This leads to the secondary objective, which is to obtain the capability to model gyroscopic effects in the FEM program Ansys. This includes a (i) natural frequency analysis that can be used to analyze how the gyroscopic effect influence the natural frequencies and the critical speeds of rotating rotors and (ii) transient analysis to analyze the effect of gyroscopic time dependent loading.

1.4 Outline

In chapter 2, the main difference between a rotating and non-rotating dynamics will be presented. Furthermore, a simple rotor configuration is considered and the governing equations are derived.

Chapter 3 provides a general introduction the modeling techniques of rotating machinery in the Finite Element Method (FEM) program Ansys. The basic steps, required to build a model which includes the rotational velocity of a component, are demonstrated with an example (the simple rotor configuration presented in chapter 2).

Next, in chapter 4 we examine how the gyroscopic effect affects the natural frequencies of two different systems. The results are compared with analytical solutions derived from the equation of motion in chapter 2. This is done to verify that the gyroscopic effect is implemented correctly in Ansys, which is the absolute keystone of this report.

In chapter 5 we perform a transient analysis. The results are, in the same manner as in chapter 4, verified with an analytical solution.

Finally, in chapter 6, we apply the model developed in chapter 3, 4 and 5 and analyze how gyroscopic effects affect the dynamic response of a floating offshore wind turbine.

1.5 References

[0.1] <http://encyclopedia2.thefreedictionary.com/Gyroscopic+Inertia>

[0.2] Serway Jewett. Physics for Scientists and Engineeris with Modern Physics, 6th Edition.

[0.3] <http://www.gyroscopes.org/behaviour.asp>

[0.4] <http://ma3naido.blogspot.com/2008/11/gyroscopic-action.html>

- [0.5] Lucy Y. Pao and Kathryn E. Johnson. A tutorial on the Dynamics and Control of Wind Turbines and Wind Farms. *2009 American Control Conference Hyatt Regency Riverfront, St. Louis, MO, USA June 10-12, 2009.* {6}.
- [0.6] A.R Henderson, R.Leutz, T. Fujii. Potential for floating Offshore Wind Energy in Japanese Waters. *International Offshore and Polar Engineering Conference Kitakyushu, Japan, May 26-31, 2002* {508}
- [0.7] Henderson, A. R. and Patel, M. H., “On the Modelling of a Floating Offshore Wind Turbine,” *Wind Energy, Vol. 6, No. 1, February 2003*, pp. 53–86.
- [0.8] Dominique Roddier , Christian Cermelli, Alla Weinstein. Windfloat: A Floating Foundation for Offshore Wind Turbines Part I: Design Basis and Qualification Process. *Proceedings of the ASME 28th International Conference on Ocean, Offshore and Arctic Engineering OMAE2009 May 31 – June 5, 2009, Honolulu, Hawaii, USA*
- [0.9] J.M. Jonkman and M.L. Buhl, Jr. Loads Analysis of a Floating Offshore Wind Turbine Using Fully Coupled Simulation. *Conference Paper NREL/CP-500-41714 June 2007.* {23}
- [0.10] http://en.wikipedia.org/wiki/Inverted_pendulum
- [1.5], [1.6], [1.7], [1.8] and [1.9] can be found on the attached CD.

2 Basic Rotor Dynamics

2.1 Preliminaries

The aim of this chapter is to introduce the basic characteristics of a rotating machinery. This is done by introducing a simple rotor model. The model consists of a single rigid disk centrally mounted on a uniform flexible massless shaft, supported by two identical rigid bearings at each side. The simple rotor model is illustrated in Figure 2.1 (a) and the coordinate system used to describe the motions of the system is illustrated in Figure 2.1 (b). The axis x , y and z , in this order, form a right-handed set.

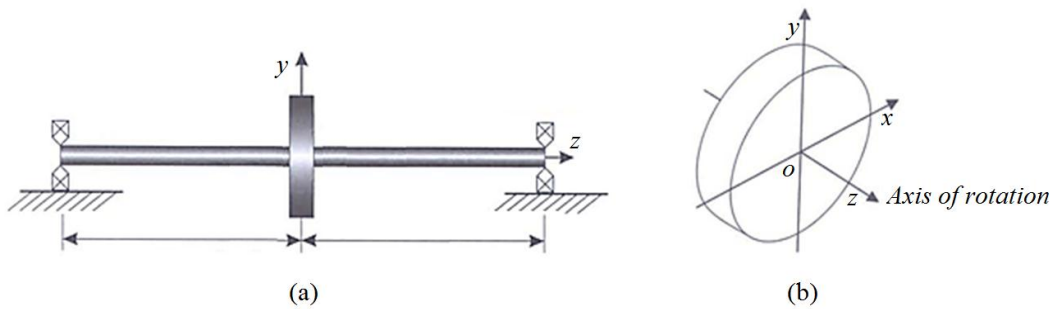


Figure 2.1 (a) A simple rotor model. (b) Right-handed coordinate system. The rotor rotates around the z -axis, [2.1].

2.1.1 Mode shapes

The simple rotor model can be considered as a mass-spring system if we assume that the rotor is not spinning, i.e. no rotation. The damping from the shaft and bearings is neglected. The vibration characteristics are determined by the systems mass and stiffness values, and the natural frequencies and mode shapes are obtained by solving the eigenvalue problem. The natural frequencies are determined from the eigenvalues and each eigenvalue is associated with an eigenvector, which represents the mode shape. The motion, associated to each frequency is planar, i.e. a movement in the z - x plane or the z - y plane. The mode shapes are illustrated in Figure 2.2. The mode shapes are illustrated in the z - x plane.

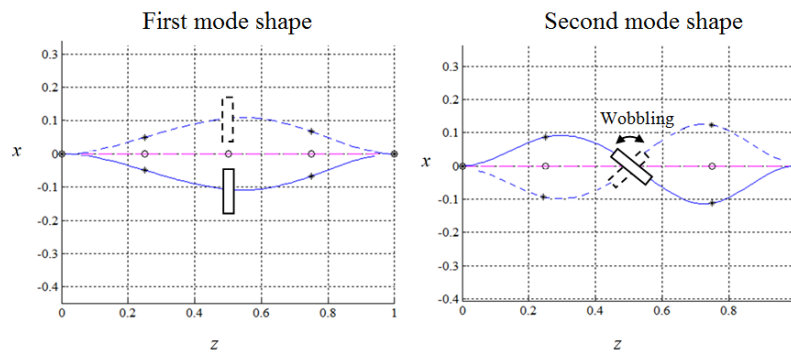


Figure 2.2 The first two mode shapes for the simple rotor system. The rotor is not rotating and the modes are a pure planar motion in the z - x plane.

The centrally mounted disk translates vertically in x direction without any wobbling at the first mode shape. The phenomenon of wobbling is illustrated in Figure 2.2 (right), where the centrally mounted disk is rocking from side to side. At the second mode shape, the vertical translation is zero and the movement is pure wobbling mode of the shaft, see Figure 2.2. If the disk were placed off-center, the movement would be a combination of translation and wobbling. The wobbling motion of the disk introduces some interesting features once the shaft starts to rotate, namely the gyroscopic effect.

The dynamics of the rotor cannot be described by a spring-mass system when the rotor starts to rotate. Although the dynamic behavior is different, it still shares the existence of natural frequencies and mode shapes. The mode shapes look similar to the nonrotating modes, see Figure 2.2, but involve a circular motion instead of planar motion, as illustrated in Figure 2.3. The circular motion is called whirling.

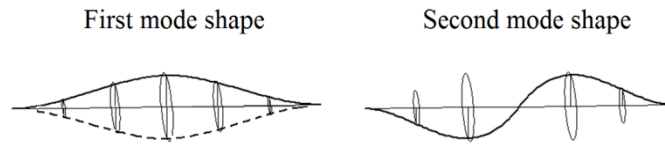


Figure 2.3 The first two mode shapes for the simple rotor system. The modes are called a cylindrical- and conical mode, respectively.

A mode shape is called a cylindrical mode if the rotor traces the outline of a cylinder. The first mode shape is characterized as a cylindrical mode. The second mode shape is called a conical mode. These motions are described with four degrees of freedom, two lateral and two rotational. $\{u\} = \{x \ y \ \theta \ \psi\}^T$, where the rotation around the x - and y axis is given by θ and ψ , respectively. These definitions are illustrated in Figure 2.4. A positive rotation in z direction is denoted Φ .

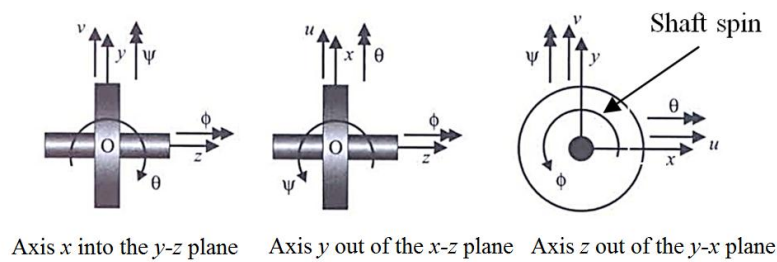


Figure 2.4 Definitions used to describe the system, [2.1].

2.1.2 Forward and backward whirling

The first mode shape is a cylindrical mode and viewed from the front it looks like the rotor is bouncing up and down. This movement can be visualized as jump rope swinging around and is called a whirling motion. The rotor is, unlike a jump-rope, also rotating. The shaft is spinning in one direction, and the whirling motion of the rotor can either be in the same direction or in the opposite direction. If the whirling motion of the rotor is in the same direction as the shaft, the

mode is called forward whirling. If the whirling of the rotor is in the opposite direction as the shaft, the mode is called backward whirling. A forward whirling increase the natural frequency and a backward whirling decreases the natural frequency [2.2]. The principle of forward and backward whirling is illustrated in Figure 2.5, where the cross section is shown over the course of time. The time is denoted T . Note the black square on the cross-section. The cross-section is moving counterclockwise for a forward whirling and clockwise for backward whirling.

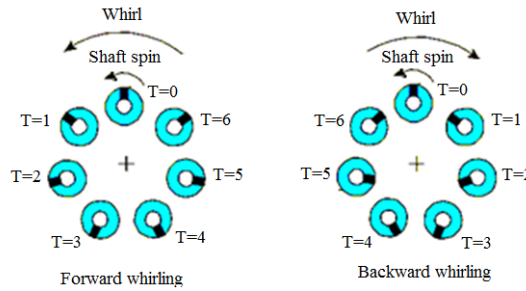


Figure 2.5: Forward- and backward whirling. A point on the surface of the rotor (black square) moves in the same direction as the whirl for a forward whirling and in the opposite direction for a backward whirling. The stiffness of the system is increased in for a forward whirling and decreased for a backward whirling, [2.2].

The second mode shape is similar to the wobbling mode shape of the nonrotating system, but involves a circular motion instead of planar motion. The conical mode shape can as the cylindrical mode shape whirl in the same direction as the shaft spin direction or in the opposite direction (forward- and backward whirling).

2.1.3 Gyroscopic Effect

The interaction of the angular momentum of the rotating rotor and the wobbling motion introduce an effect called the gyroscopic effect. The gyroscopic effect is only observed for modes which includes an angular (wobbling) component. The gyroscopic effect implies a change in the stiffness of the system, which means that the natural frequency also changes. A forward whirling increases the stiffness of a system while backward whirling decreases the stiffness of a system [2.2].

A frequency map, is a graphically way to illustrate the influence of the gyroscopic effect on the natural frequencies. The rotational speed is plotted on the x-axis and the natural frequency on the y-axis. This is also called a Ω - ω diagram.

2.1.4 Critical speed - Ω - ω diagram

Forces in rotating machine may occur due to misalignments, a bended rotor, or due to a certain imbalance in the rotating disk. Machines are designed on the basis of manufacturing tolerances, and the imbalance can in principle be as small as one wish, but obviously this is related to the costs of the machine. This means there will always be small imbalance. An imbalance can also be introduced due to wear of machine part. An imbalance causes lateral forces whose frequencies

are locked to the rotor speed. If the frequency of the force is equal the rotor speed the force is said to be synchronous. This produces a straight line of positive slope in the Ω - ω diagram, and is referred to as the one-times spin speed and labeled 1X. The intersection of the synchronous line with the forward- and backward whirling curves is analog to resonance in a stationary system. Resonance is associated with a local peak in amplitude and a shift in phase. The term resonance is not used for a rotating system, but the principle is the same, only with the substitution of the term critical speed for resonance.

A Ω - ω diagram and an unbalance response diagram are illustrated in Figure 2.6. The system which forms the basis of these plots is axial symmetrical, i.e. the stiffness is the same in the x - and y - axis. The rotor is placed along the z -axis. The disk is placed off center, which results in a wobbling for both the first- and second mode shape. This explains why the first natural frequency separates. There is no damping in the shaft and the response is tending to infinity.

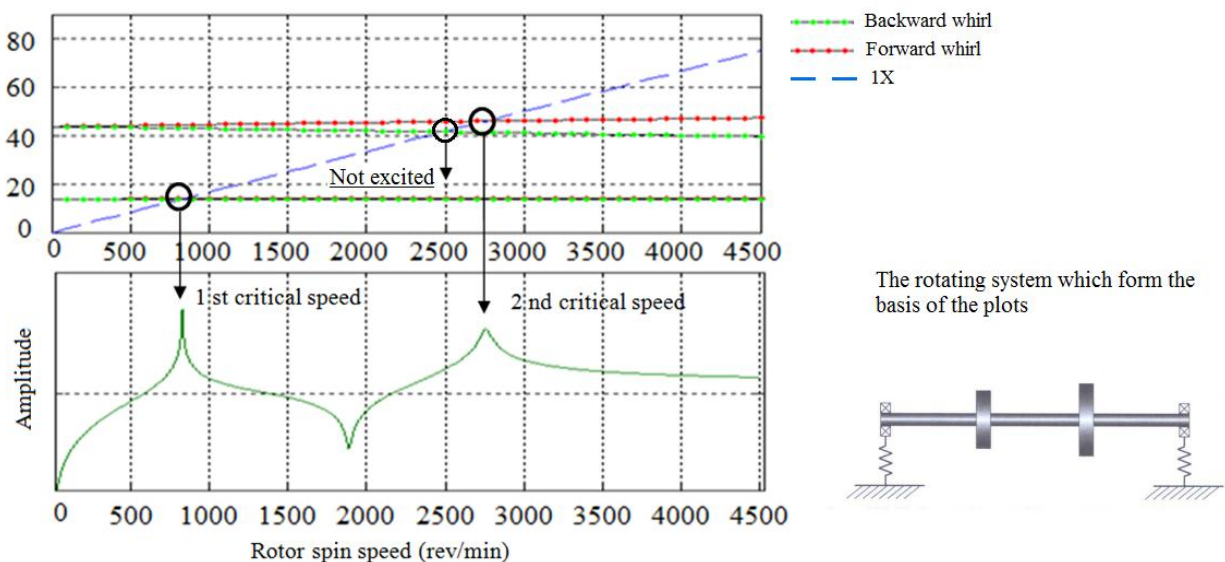


Figure 2.6: Comparison between natural frequencies and critical speeds. Top: Ω - ω diagram. Bottom: Unbalance response diagram. The plots are made with a Matlab code from [2.1] Attached on the CD.

With reference to statically dynamics it is expected that each intersection implies a critical speed. This is immediately not the case for an axisymmetric rotor. The modes are circular, and either purely forward-whirling or purely backward whirling modes. The unbalance force does not excite the backward-whirling modes, even though the synchronous line intersects the backward frequency before the forward whirling mode.

A generic term called “Critical speed analysis” is often used in rotor dynamics. The meaning of this term is to perform an analysis in order to identify the critical speeds of a machine. The critical speed can be identified with both a modal analysis and a forced response analysis. A critical speed should always be avoided in any machines parts because otherwise significant vibrations may occur. These vibrations are the result of a resonant condition.

The purpose of the natural frequency analysis is to compute the natural frequencies of the rotor system. The calculated natural frequencies can then be used to determine the critical speeds of the machine. Rotors have natural frequencies corresponding to both forward- and backward whirling, see section 2.1.2. The backward whirling often do not produce a critical speed. This means that using a modal analysis to identify critical speeds is not always straight forward.

Forced response analysis is used to produce a response diagram of a displacement versus machine speed. The plots can be used compare experiments (field measurements) and numerical models. The critical speeds can be determined in a very direct fashion by identifying local peaks in the response diagram.

In summary, this means that a blend of natural frequency analysis and forced response analysis is the best and most reliable way to determine critical speeds of a system. The following procedure can be used to determine critical speeds:

- **Perform a natural frequency analysis** to determine the natural frequencies and mode shapes of the system. The natural frequencies can be used predict the probable locations of the critical speeds. The mode shapes related to each natural frequency is used to dictate how to apply the excitation force in a subsequent forced response analysis.
- **A forced response analysis** is then performed to check how structure reacts when the excitation frequency equals the natural frequency. The speed is deemed a critical speed if the response is sufficiently¹ severe.

The response obtained by a forced response analysis is independent of the time and does not provide any information about how resonant growth in time. This is interesting during a startup (acceleration) or a shutdown of a rotor system where critical speeds are passed over a short period of time. However, this information can be achieved by a transient analysis where the loads can be added as time-dependent functions, i.e. a ramped rotational velocity over a given a time period to simulate a startup or a shutdown.

2.2 A simple rotor model – Governing equations

The aim of this section is to derive the governing equations for a simple rotor model. These equations are then solved analytically in the next following chapters and compared with a similar

¹ A critical speed is according to “The American Petroleum Institute (API)” , in API publication 684, defined as rotational speed that corresponds to the peak of a non-critically (amplification factor $> 2,5$) damped rotor system frequency

model in the finite element program Ansys. The motion of the disk is described with four degrees of freedom, two laterals and two rotational. $\{u\} = \{x \ y \ \theta \ \psi\}^T$.

2.2.1 Equations of motion – lateral modes

The disk has a mass of m and the center of gravity offset from the shaft center is defined by an eccentricity ε , as shown in Figure 2.7. It is assumed that the damping of the shaft is zero.

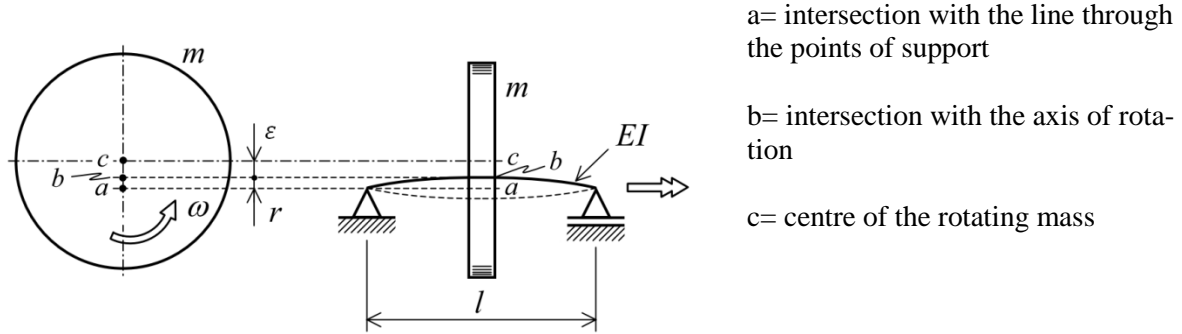


Figure 2.7 Rotating mass on a flexible shaft.

The distance bc is indicated as ε and the distance ab as r , where ε is the eccentricity and r is the deflection of the beam. The position of the mass center, see Figure 2.7 (point c) is initially described by one degree of freedom, i.e. as a radial motion. The equation of motion for the mass center is derived from Newton's second law

$$m \frac{d^2}{dt^2} (r + \varepsilon) = -kr, \quad (2.1)$$

where k is the bending stiffness of the shaft. The position of the mass center expressed in the x - y coordinate system is illustrated in Figure 2.8.

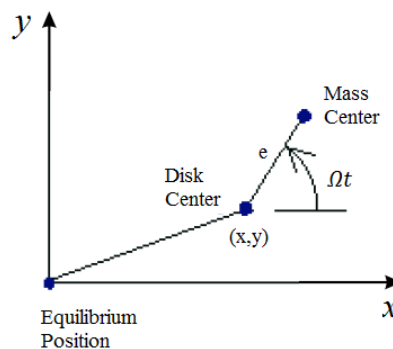


Figure 2.8 Position of the bearing centerline (disk center) and the rotor mass center.

The equations of motion is then, in the x - y coordinate system, given by

$$m \frac{d^2}{dt^2} (x + e \cos(\Omega t)) = -K_x x, \quad (2.2)$$

$$m \frac{d^2}{dt^2} (y + e \sin(\Omega t)) = -K_y y. \quad (2.3)$$

Rewritten as

$$m \ddot{x} + K_x x = m \varepsilon \Omega^2 \cos(\Omega t), \quad (2.4)$$

$$m \ddot{y} + K_y y = m \varepsilon \Omega^2 \sin(\Omega t). \quad (2.5)$$

The cylindrical modes are described by the degrees of freedom U_x and U_y . It can be seen that the equations of motion in the x - and y direction are decoupled for this simple rotor system. The system is coupled when a rotational motion of the disk is included. There are no terms on left side of (2.4) and (2.5) that involve the rotational speed Ω which indicates that the natural frequencies are independent of rotor spin-speed. This immediately not the case when the wobbling motion of the rotor is included in equations of motion.

The gyroscopic effect, due to the wobbling motion, is included in the equation of motions by considering a rotation of the disk about x and y axes.

2.2.2 Angular momentum

The angular momentum L_z of the rotor about the z axis is given by $I_p \Omega$. The disk has a polar mass moment of inertia I_p and a transverse moment of inertia. The transverse moment of inertia is called the diametral moment of inertia I_d . There is a relation between I_p and I_d , defined by $I_p = 2I_d$. The polar moment inertia I_p is a quantity used to describe an object's ability to resist torsion and the diametral moment of inertia I_d characterizes an object's angular acceleration due to a torque.

Initially, the disk rotates around the y axis with an angular velocity $\dot{\psi}$ over the time δt , as shown in Figure 2.9. The rotation angle of the disk, under assumption of small displacements is $\delta\psi = \dot{\psi} \delta t$. The magnitude of the angular momentum L_z is due to conservation of angular momentum, at the end of this time period δt still $I_p \Omega$ but it is due to wobbling rotated with an angle $\delta\psi$.

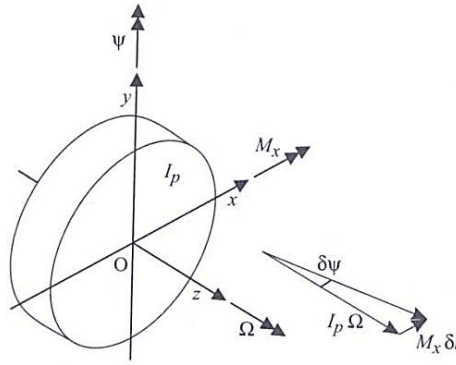


Figure 2.9 Vector representation of the effect of clockwise moment about Ox . [2.1]

An infinitesimal rotation $\delta\psi$ of the disk around the y axis, courses a vector change in angular momentum in the direction of the x axis with a magnitude $M_x\delta t$, where M_x is the clockwise moment about the x -axis, expressed as

$$M_x\delta t = I_p\Omega\sin(\delta\psi). \quad (2.6)$$

The moment M_x can under the assumptions of small rotations $\sin(\delta\psi) \approx \delta\psi$ and dividing by δt be written as

$$M_x = I_p\Omega \frac{\delta\psi}{\delta t}, \quad (2.7)$$

and taking the limit $\delta t \rightarrow 0$, we have

$$M_x = I_p\Omega\dot{\psi}. \quad (2.8)$$

The same principles are valid for a rotation around the x axis. If the disk rotates around the x axis with an angular velocity $\dot{\theta}$ during the time δt , the rotation angle of the disk is, under assumption of small displacements $\delta\theta = \dot{\theta}\delta t$. The change in angular momentum L_z is in the negative y direction. Thus, the vector $-M_y\delta t$ is negative and M_y is a clockwise moment about the y -axis, given by

$$M_y\delta t = -I_p\Omega\sin(\delta\theta). \quad (2.9)$$

Figure 2.10 shows the principle described above but with a negative rotation around the x axis, which results in a positive vector $M_y\delta t$.

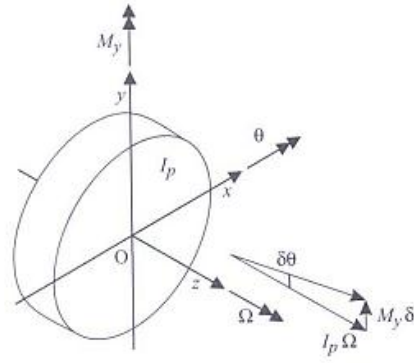


Figure 2.10 Vector representation of the effect of a counter clockwise moment about Oy. [2.1]

Thus, M_y can under the assumptions of small rotations $\sin(\delta\theta) \approx \delta\theta$ and dividing by δt and $\delta t \rightarrow 0$ be written as

$$M_y = -I_p \Omega \dot{\theta}. \quad (2.10)$$

Finally, a contribution needs to be added to (2.8) and (2.10) because of the rotation of the disk about the x - and y axis.

$$M_x = I_d \ddot{\theta} + I_p \Omega \dot{\psi} \quad \text{and} \quad M_y = I_d \ddot{\psi} - I_p \Omega \dot{\theta} \quad (2.11)$$

where I_d is the diametral moment of inertia.

2.2.3 Derivation of the stiffness matrix

The equations of motion for the simple rotor model with four degree of freedom can be established when the contribution from rotation degrees of freedom are included in the stiffness matrix. The beam theory for slender beams is used to establish the relation between displacements, rotation and the applied forces; this is demonstrated in appendix A, page 60. The stiffness matrix is given below

$$[K] = \begin{pmatrix} k_1 & 0 & 0 & k_2 \\ 0 & k_1 & -k_2 & 0 \\ 0 & -k_2 & k_3 & 0 \\ k_2 & 0 & 0 & k_3 \end{pmatrix}. \quad (2.12)$$

2.2.4 Equations of motion for the complete system

The equation of motions for the complete system is obtained by combining the equations for the translational degrees of freedom (2.4) and (2.5) with the equations including the gyroscopic effect (2.11).

$$(2.13)$$

$$\begin{pmatrix} m & 0 & 0 & 0 \\ 0 & m & 0 & 0 \\ 0 & 0 & I_d & 0 \\ 0 & 0 & 0 & I_d \end{pmatrix} \begin{pmatrix} \ddot{x} \\ \ddot{y} \\ \ddot{\theta} \\ \ddot{\psi} \end{pmatrix} + \left(\Omega \begin{pmatrix} 0 & 0 & 0 & 0 \\ 0 & 0 & 0 & 0 \\ 0 & 0 & 0 & I_p \\ 0 & 0 & -I_p & 0 \end{pmatrix} \right) \begin{pmatrix} \dot{x} \\ \dot{y} \\ \dot{\theta} \\ \dot{\psi} \end{pmatrix} + \begin{pmatrix} k_1 & 0 & 0 & k_2 \\ 0 & k_1 & -k_2 & 0 \\ 0 & -k_2 & k_3 & 0 \\ k_2 & 0 & 0 & k_3 \end{pmatrix} \begin{pmatrix} x \\ y \\ \theta \\ \psi \end{pmatrix} = m\epsilon\Omega^2 \begin{pmatrix} \cos(\Omega t) \\ \sin(\Omega t) \\ 0 \\ 0 \end{pmatrix}$$

where $I = \frac{\pi d^4}{64}$, $I_d = \frac{mD^2}{16}$, $I_p = \frac{mD^2}{8}$, $k_1 = \frac{12EI}{L^3}$, $k_2 = \frac{6EI}{L^2}$, $k_3 = \frac{4EI}{L}$. d is the diameter of the shaft. D is the diameter of the disk.

There is an elastic coupling (k_2) between the first and the fourth equations as well as the second and the third equations. Furthermore, there is a gyroscopic coupling between the third and fourth equations. The elastic coupling k_2 vanish in the simple rotor model because the disk is centrally mounted on the shaft. The natural frequency related to the first mode shape is then independent of the gyroscopic effect (no wobbling).

The equation of motion (2.13) is a coupled differential equation and the solution is obtained by combination of homogeneous- and a particular solutions. A homogeneous solution is obtained by setting the right hand side of (2.13) to zero. The homogeneous solution (free response) of equation (2.13) is considered in chapter 4.

2.3 Summery

The first two mode shapes has been illustrated for a non-spinning- and a spinning rotor configuration and the principle of forward and backward whirling has been explained. It has been demonstrated, with an example, that a mode shape which includes an angular (wobbling) component introduces a gyroscopic effect. This gyroscopic effect implies a change in the stiffness of the system, which means that the natural frequency also changes. A forward whirling increases the stiffness of a system while backward whirling decreases the stiffness of a system. The equation of motion has been derived for a simper rotor configuration. This equation is solved analytically in chapter 4 where a natural frequency analysis is performed. The purpose of the analytical solutions is to verify the Ansys analysis.

2.4 References

[2.1] Michael I. Friswell et al. Dynamics of rotating machines, 1 edition 2010. {79}

[2.2] Erik Swanson, Chris D. Powell, Sorin Weissman. A Practical Review of Rotating Machinery Critical Speeds and Modes.

[2.2] can be found on the attached CD.

3 Ansys – Preprocessor

The Finite Element program Ansys is used to simulate and analyze the dynamic behavior of rotating machinery in this thesis work. Ansys offers two main types of graphical user interface, Ansys Classic and Ansys Workbench. Ansys Workbench has a modern work environment. However, Ansys Workbench does not the same rotor dynamic features that that Ansys Classic has. Ansys Classic can be used with two different techniques; one is to use the menus in the program, or to use batch files. A batch file is a text file with commands. The advantage of the batch file technique is that an entire model, mesh and solution description can be obtained in a file of 10-100KB. Interactive use requires the user to save the model geometry and mesh in *.db file and the result in a *.rst file. The *.db file can be as large as 30MB or more². The batch file technique is used in this thesis work.

3.1 Presenting the Reference Model

The aim of this section is to give a general introduction to modeling techniques relevant to rotor dynamics analysis in Ansys version 12. This is done by introducing a simple example, see Figure 3.1. The model consists of a single rigid disk centrally mounted on a uniform flexible massless shaft, supported by two identical rigid bearings at each side. The damping of the shaft and bearings is assumed to be zero.

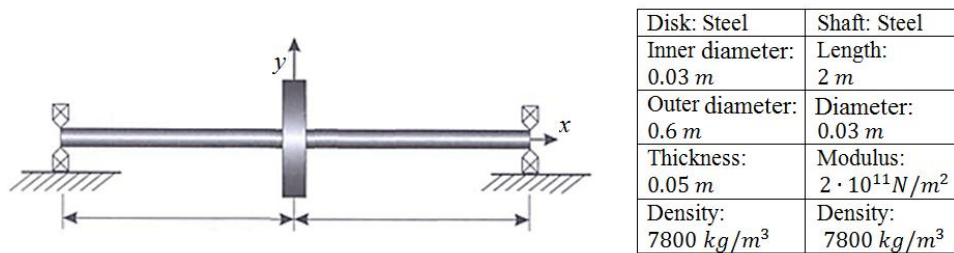


Figure 3.1 Simple rotor configuration, [3.1].

The simple rotor configuration, shown in Figure 3.1, is used to verify Ansys. This is done by comparing the Ansys results from a natural frequency analysis (chapter 4) and a transient analysis (chapter 5) to analytical solutions. The governing equations have been derived analytically in the previous section. The analytical solutions are derived from equation (2.13) (equation of motion for the simple rotor configuration).

It is not straightforward to build the geometry for a rotor dynamic analysis because the geometry has to be grouped into a rotating part and a stationary part. This is demonstrated in the following section where we define the geometry for the rotor configuration shown in Figure 3.1.

² Based on own experience from previous projects.

Rotating systems can be analyzed in a stationary- or a rotating reference frame. A stationary reference frame should be used if a rotating structure (rotor) is modeled along with a stationary support structure which is the case for all analysis in this thesis work. The difference between a stationary- and a rotating reference is explained in appendix B, page 61.

The equation of motions for the stationary reference frame is given in equation (3.1) [3.2].

$$[M]\{\ddot{u}\} + ([C] + [C_{gyr}])\{\dot{u}\} + [K]\{u\} = \{F\}, \quad (3.1)$$

where $[M]$ is mass matrix, $[K]$ is stiffness matrix, $[C]$ is damping matrix, and $[C_{gyr}]$ is gyroscopic matrix. Equation (3.1) is similar to equation (2.13) derived in chapter 2, section 2.2.4.

3.2 Building the Model - Preprocessor

Building a model for a rotor dynamic analysis consists of several steps. The purpose of the following section is to describe how the geometry can be defined, by the batch file method, for the model presented in section 3.1. The material parameters are initially defined in the batch file below (grey rectangular box). The LGW file can be found on the attached CD [LGW_1].

Code:

! ** Material steel	
mp,ex,1,2.0e+11	! Modulus of elasticity
mp,nuxy,1,0.3	! Poisson ratio
mp,dens,1,7800	! Density

The next thing that has to be defined is the element types. The shaft is modeled with the 3D beam element, BEAM188. The disk is modeled with a mass element, MASS21. This element type requires six real constant input values, a mass in the x , y and z -direction direction and a mass moment of inertia in the x , y and z -direction. The polar mass moment of inertia I_p is defined in the x - direction and the diametral moment of inertia I_d is defined in the y and z -direction.

Code:

! ** Element types shaft	
et,1,188,,2	! Element type 1= 3D beam element
sectype,1,beam,csolid	! Associates the beam element with a circular cross section
secddata,0.015,8	! Defines the diameter and element division of cross section
! ** Element types disk	
et,2,21	! Element type 2= MASS21 element
md=110	! Defines the mass
ip=4.95	! Defines the polar mass moment of inertia
id=2.475	! Defines the diametral mass moment of inertia
r,3,md,md,md,ip,id,id	! Defines the real constants for the MASS21 element

The nodes are then defined.

Code:

! ** Nodes	
n,1	! Define node 1 at location x=0, y=0, z=0
n,2 ,0.5	! Define node 1 at location x=0.5, y=0, z=0
n,3 ,1.0	! Define node 1 at location x=1, y=0, z=0
n,4 ,1.5	! Define node 1 at location x=1.5, y=0, z=0
n,5 ,2.0	! Define node 1 at location x=2, y=0, z=0

The elements are then defined and associated with the right element type.

Code:

! ** Associate the elements to the right nodes	
type,1	! Selects element type 1 (BEAM 188)
secn,1	! Selects section number 1 (circular cross section)
e,1,2	! Defines an element between node 1 and 2
e,2,3	! Defines an element between node 2 and 3
e,3,4	! Defines an element between node 3 and 4
e,4,5	! Defines an element between node 4 and 5

The rigid disk is located at node 3 which is located at the midpoint of shaft.

Code:

type,2	! Selects element type 2 (MASS21)
real,3	! Selects real constant set nr. 3
e,3	! Defines the element by node connectivity

It is important to identify and separate rotating and non-rotating part when building a model for a rotor dynamic analysis in order to apply the rotational velocity (or velocities) to the rotating part. All rotating parts are (shaft + disk) grouped into one component, called shaft, with the following command.

Code:

CM,shaft,elem	! All elements grouped into one component called shaft. This is the part of the structure that rotates!
---------------	--

Finally, boundary conditions are applied to the model.

Code:

```
d,1,all  
d,5,all  
d,all,ux      ! supress axial motion      ! supress axial motion  
d,all,rotx
```

The plot of the geometry is shown in Figure 3.2.

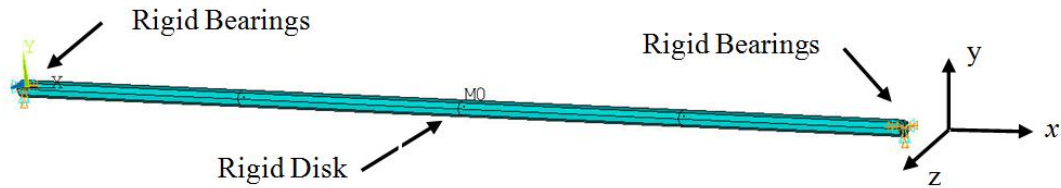


Figure 3.2 Geometry of the example. The example is modeled with four BEAM188 elements (3D elements) and two. The rigid disk is modeled with a MASS21 element.

3.3 Summery

A simple rotor configuration is presented. The geometry has been modeled with the batch file method. The most important command is the 'CM' command which groups the elements into one component. It is possible, with this command, to divide a structure into different parts and then assign a rotational velocity to each part.

3.4 References

[3.1] Michael I. Friswell et al. Dynamics of rotating machines, 1 edition 2010. {79}

[3.2] Rotordynamic analysis Guide, Release 12.0, April 2009. {7}

[3.2] can be found on the attached CD.

4 Natural frequency Analysis

The purpose of this chapter is to explain the steps required to perform a natural frequency analysis in Ansys where the gyroscopic effect is included. A natural frequency analysis is performed in Ansys and validated by comparing the result against a corresponding analytical solution. The numerical and analytical solution is based on the rotor configuration presented in the previous section. The analytical solution is derived from the equation of motions in chapter 2.

Secondly, a parameter study of an overhang rotor configuration is carried out and we examine how the overhang length and the diameter of the rotating disk affect the gyroscopic effect. Third, a combined system consisting of a rotor configuration and an underlying stationary support structure is considered and we analyze how the gyroscopic effect influences the natural frequencies of this combined system.

4.1 Natural Frequency Analysis in Ansys

The fundamental difference between a traditional natural frequency analysis (no rotation) and a natural frequency analysis dealing with rotor dynamics is that spinning components adds additional forces to the system due to gyroscopic effects. The gyroscopic effect is included by executing the command ‘CORIOLIS,on,,,on’ [4.1]. The coriolis command applies the coriolis/gyroscopic effect of a rotating structure. The rotational velocity of the rotating component is defined using the CMOMEGA command. The CMOMEGA command recognizes all rotating part provided that these are grouped into one component. This is done with the CM command, as explained in the chapter 3.

Regular eigen solvers like Subspace, Block Lanczos cannot be employed because the inclusion of the gyroscopic effect result in a non-symmetric damping matrix, and therefore require a non-symmetric solver. The eigen solver DAMP and QRDAMP in Ansys can be used to the unsymmetrical eigenvalue problem [4.1]. The QR damped method allows both nonsymmetric [K] and [C] matrices. The solver is computationally efficient compared to damp eigensolver [4.2]. The QR damped solver is used in this thesis work and the command ‘modopt,qrdamp, , ,on’ is used to activate the solver.

The Ω - ω diagram, which is used to plot the rotational speed Ω versus natural frequency ω , is produced by introducing a loop and repeating the solver procedure for different rotational speeds. The batch file below shows how to set up the solver for this kind of a natural frequency analysis. The solution procedure is applied to the example/geometry presented in Chapter 3 and compared to an analytical solution. This is done in section 4.3.

Natural frequencies are calculated in a frequency interval between 0-1000 rpm. The rotational velocity is increased with 100 rpm. at each load step.

Code:

/SOLU	
CORIOLIS,on,,,on	! Include the Coriolis effect in a stationary reference frame
pi=acos(-1)	! Defines pi
neigv=4	! Number of modes to expand
nint=11	! Numbers of load steps
speeddel=100	! The load step size, i.e. the first calculation starts at 0 rpm and the next is then calculated at 100 rpm. The final load step is 1000 rpm. (nint=11)
antype,modal	! The analysis type is a modal analysis
modopt,qrdamp,neigv,0.1,,on	! Specifies the natural frequency analysis options. a complex solver is used for the damped system
*do,i,1,nint	! Loops over the load steps (100 rpm in each load step)
spn=(i-1)*speeddel*2*pi/60	! Defines the rotation speed in rad/s
CMOMEGA,shaft,spn,,,0,0,0,2,0,0	! Specifies the rotational velocity of an element component (shaft) about a user-defined rotational axis (x-axis)
mexpand,neigv	! Specifies the number of modes to expand
solve	! Solves the system
*enddo	! End loop
FINISH	

The Ω - ω diagram is plotted with the following commands and shown in Figure 4.1 in section 4.3.

Code:

/post1	
plcamp,,1,rpm,,shaft	! plot of the Ω - ω diagram (also called a Campbell diagram)
prcamp,,1,rpm,,shaft	! Forward and backward whirls are printed out in a table

Results are presented in section 4.3.

4.2 Natural Frequency Analysis - Analytical Solution

The natural frequencies of the system are obtained by setting the right hand side of equation (2.13) to zero (equation of motion). The elastic coupling k_2 , in equation (2.13), vanish because the disk is centrally mounted on the shaft and the equation of motions yields

$$m\ddot{x} + k_1x = 0 \quad (4.1)$$

$$m\ddot{y} + k_1y = 0 \quad (4.2)$$

$$I_d\ddot{\theta} + I_p\Omega\dot{\psi} + k_3\theta = 0 \quad (4.3)$$

$$I_d\ddot{\psi} - I_p\Omega\dot{\theta} + k_3\psi = 0 \quad (4.4)$$

The derivation of the natural frequencies is given in Appendix C, page 62, and the result is given below.

$$\left. \begin{aligned} \omega_1 &= \omega_2 = \sqrt{\frac{k_1}{m}}, \\ \omega_3 &= -\frac{I_p \Omega}{2I_d} + \sqrt{\left(\frac{I_p \Omega}{2I_d}\right)^2 + \frac{k_3}{I_d}}, \\ \omega_4 &= \frac{I_p \Omega}{2I_d} + \sqrt{\left(\frac{I_p \Omega}{2I_d}\right)^2 + \frac{k_3}{I_d}}. \end{aligned} \right\} \quad (4.5)$$

It can then be seen that the natural frequency ω_3 is decreasing with increasing rotational speed, and

ω_4 is increasing with increasing rotational speed. This behavior is due to the influence of the gyroscopic effect which is caused by the wobbling of the disk. Equation

(4.5) can be used create a Ω - ω diagram.

4.3 Comparison – Numerical and Analytical Solution

The result from the modal analysis, based on the analytical solution and Ansys, is plotted in a Ω - ω diagram, see Figure 4.1. The LGW file can be found on the attached CD [LGW_2] and the Matlab plotting routine [Matlab_1].

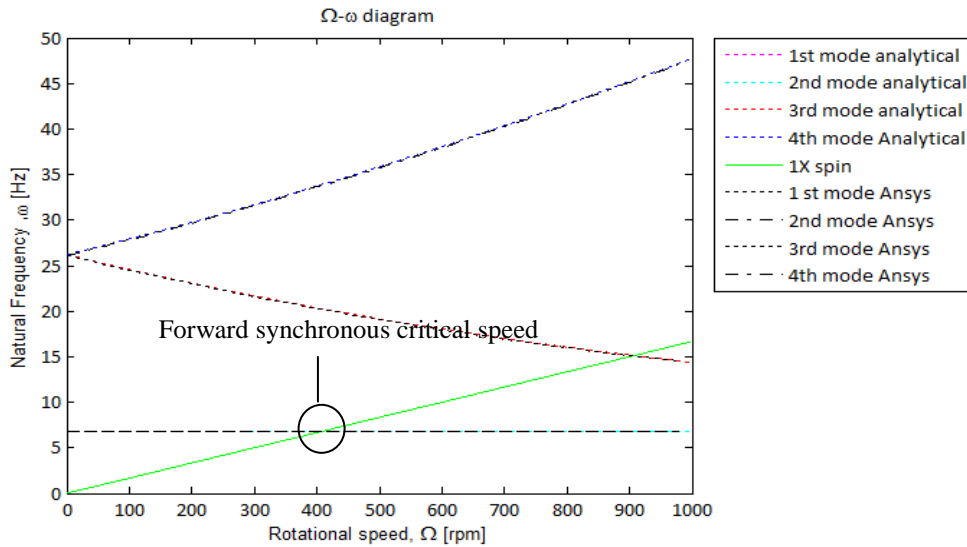


Figure 4.1: Ω - ω diagram for the analytical and Ansys solution.

The first and second mode is independent of the rotational speed and does not separate. This is because disk does not have any wobbling motion, which is needed to get an influence from the gyroscopic effect. The 3rd mode is a backward whirling and natural frequency is decreasing as the rotational speed is increasing. The 4th mode is a forward whirling and the natural frequency is

increasing as the rotational speed is increasing. The excitation line (green) is denoted 1X spin. The result from the analytical solution and Ansys is the same.

There are three intersections between the excitation line and the forward- and backward whirling curves, two at 400 rpm and one at 900 rpm, where the latter is a backward whirling. The first forward mode which crosses the excitation line at 400 rpm is a critical speed. The next intersection is not a critical speed because backward whirling modes are not excited. This is demonstrated in Appendix H, page 74, where the system is analyzed for unbalance forces in the frequency range 0-1000 rpm. This type of analysis is called a harmonic analysis.

4.4 Parameter Study of an Overhang Rotor

It was shown in the previous section that natural frequencies were affected by the gyroscopic effect. The purpose of this section is to analyze which parameters affect the gyroscopic effect. An overhang rotor configuration is initially considered. In a parameter study we analyze how the overhang length and the diameter of the rotating disk affect the gyroscopic effect. Finally, in section 4.4.4, we couple the overhang rotor configuration to a stationary structure and analyze how the gyroscopic effect affects this combined system.

The gyroscopic effect implies a change in the stiffness of the system which changes the natural frequencies. Natural frequency vs. rotation speed diagrams, Ω - ω diagram, is in the following analysis used as a measure of the gyroscopic effect.

4.4.1 Overhang Rotor Configuration

We analyze a rotor configuration, in which a part of the rotor is located outboard of the bearing supports. Such a rotor system is called an overhang rotor system and is often observed in turbochargers, fans and wind turbines. Examples of overhang rotor configurations are shown in Figure 4.2.

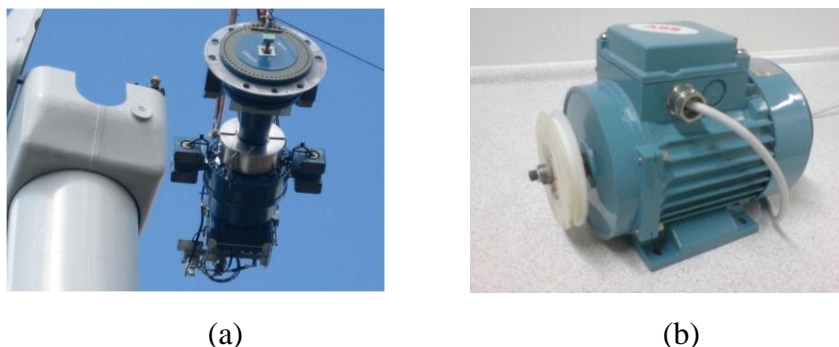


Figure 4.2 (a) Wind turbine rotor [4.3]. (b) A 0.3 KW motor with an overhang rotor configuration.

Rotating structures are always attached to static structures through some kind of bearings. The system can be visualized as a system supported by springs. The spring stiffness may depend on

the velocity and vary in each bearing. The motor (overhang rotor configuration) shown in Figure 4.2 (right) forms the basis of the following analysis. The overhang rotor configuration is modeled in Ansys with 17 3-D beam elements, see Figure 4.3, and supported by two springs. The springs are modeled with COMBI214 elements, which is an element with longitudinal as well as cross-coupling capability in 2-D applications. This element is further described in appendix D, page 65. The spring-elements are located in the y - z plane. A disk is placed at the end of the overhang. The disk cannot be plotted because it not physically modeled. The disk is added as a point element (MASS21). This element type requires six real constant input values, a mass in the x , y and z -direction and a mass moment of inertia in the x , y and z -direction. The polar mass moment of inertia I_p is defined in the x -direction and the diametral moment of inertia I_d is defined in the y and z -direction.

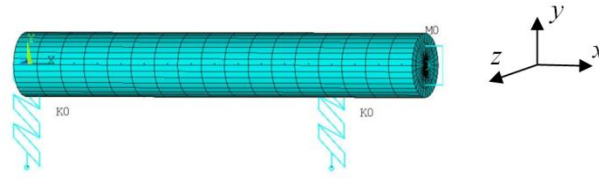


Figure 4.3: Beam model in Ansys. The span between the supports is 130 mm and the overhang length is 40 mm. The shaft diameter is 25 mm.

We examine how the overhang length and the diameter of the rotating disk affect the gyroscopic effect.

4.4.2 Influence of the Overhang Length on the Natural Frequencies

The influence of the overhang length on the natural frequencies is analyzed by comparing two rotor configurations with 40- and 80 mm overhang, respectively. The models are supported on rigid bearings. The influence of the overhang length on the first and second natural is shown in Figure 4.4. The LGW files can be found on the attached CD [LGW_3] (short rotor) and [LGW_4] (long rotor) and the Matlab plotting routine [Matlab_2].

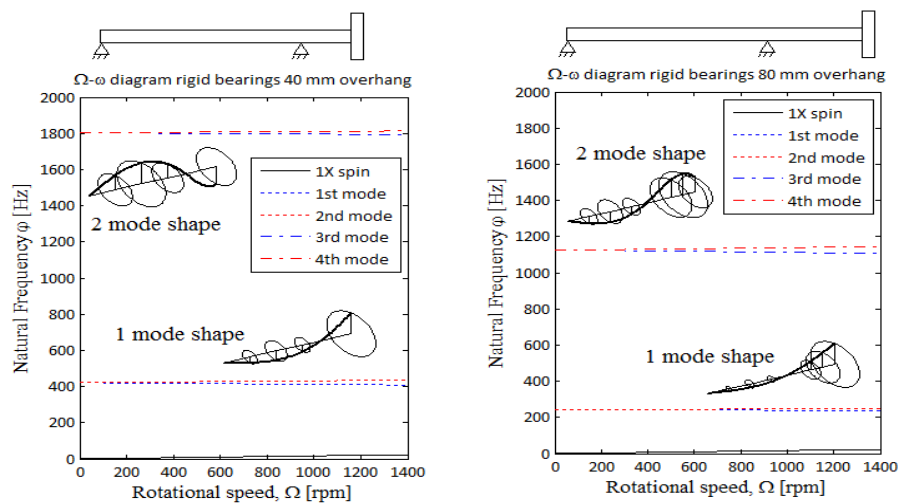


Figure 4.4: Ω - ω diagram for a rotor configuration with 40 mm overhang and a rotor configuration with 80 mm overhang, supported on rigid bearings.

The natural frequency drops as the overhang length increases, because the stiffness of the shaft decreases as the overhang length increases. Increasing the overhang length results in an increased gyroscopic effect for the 3rd and 4th mode, i.e. the separation between the forward and backward whirling frequency is larger for Figure 4.4 (right) compared to Figure 4.4 (left). The opposite behavior is observed for the 1st and 2nd mode.

4.4.3 Influence of Different Disk Properties on the Natural Frequencies

The influence of different disk properties is analyzed. A rotor system called nominal, is compared with a rotor system with the same the same diameter disk but with a two times heavier disk. The system is also compared with a system that has the same weight but the disk thickness is half of the nominal. This result in a disk diameter 1.34 times the nominal. As a result, the diametral moment of inertia and a polar moment of inertia is increased with a factor 2. Figure 4.5 shows the three models and the respective Ω - ω diagram diagrams. The models is supported on intermediate bearings, $k = 10^6$ N/m. The LGW files can be found on the attached CD [LGW_5] (Nominal), [LGW_6] (heavier disk) and [LGW_7] (large diameter) and the Matlab plotting routine [Matlab_3]

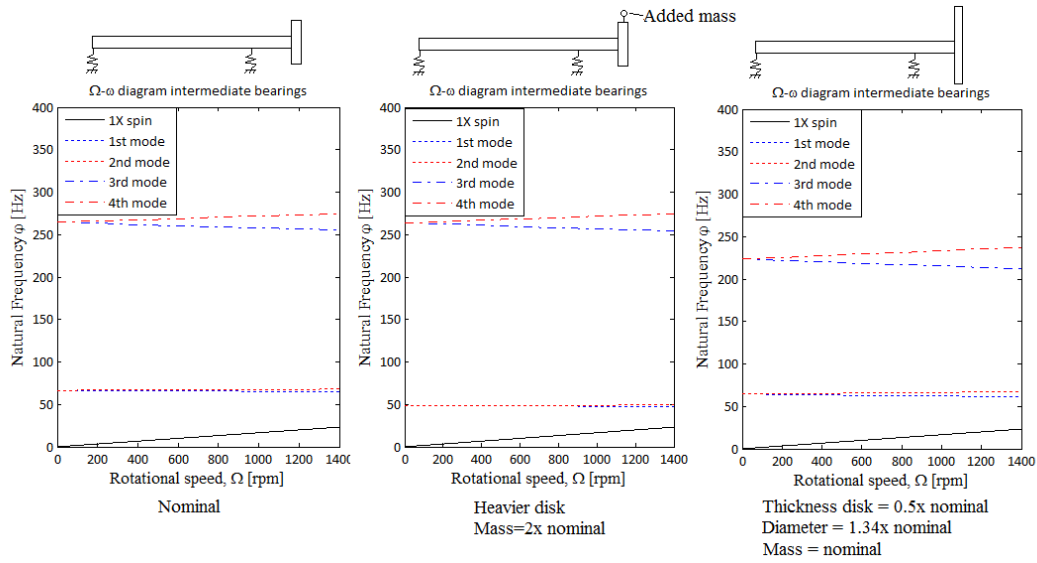


Figure 4.5: Ω - ω diagram for a rotor configuration with different disk properties.

Figure 4.5 shows the following; The added mass lowers the first mode frequencies because it is a point of large whirling motion. The added mass does not affect the second mode frequencies. The increased diametral moment of inertia and a polar moment of inertia imply a small decrease in the natural frequencies for the 1st and 2nd modes and a large decrease for the 3rd and 4th modes. A large disk increase the gyroscopic effect for all modes, this can be seen by comparing the separation between the backward and forward frequencies Figure 4.5 left and Figure 4.5 right.

We have shown that the gyroscopic effect influence the natural frequencies of a simple rotor configuration. Furthermore, it has been demonstrated that the gyroscopic effect is most dominating for modes which involves a large wobbling motion, i.e. the gyroscopic effect increase when the overhang length increases. We will in the following section couple the rotor configuration to a stationary structure and analyze how the gyroscopic effect affects the natural frequencies a combined system.

4.4.4 Coupling of a Stationary Structure and a Rotor Configuration

A combined systems consisting of a rotating shaft and an underlying stationary support structure is analyzed in this section. The rotating shaft introduces a gyroscopic effect that adds additional forces into the systems that course the natural frequencies to change as a function of the rotational speed. This means that the natural frequency of the stationary structure can be changed, but this requires that the gyroscopic effect is strong enough to affect the stiffness of the stationary structure.

A combined system, shown in Figure 4.6, is considered. The system consists of the overhang rotor configuration used in the previous section attached to a stationary structure with springs. The springs are modeled with COMBI214 elements, which is an element with longitudinal as well as cross-coupling capability in 2-D applications. The spring-elements are located in the y-z plane. These springs are in the following called rotor-springs. The stationary structure is modeled with beam elements that are supported by four springs in each corner. These spring-elements are located in the y-z plane and denoted support-springs.

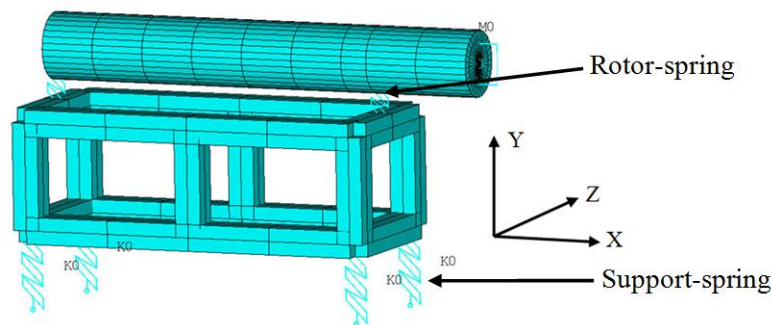


Figure 4.6: Overhang rotor configuration supported on a stationary structure.

It is known from previous analysis that the gyroscopic effect is most dominating for modes that involve a large wobbling motion of the disk. This is achieved if support springs are made very soft. The mode shapes are shown in Figure 4.7.

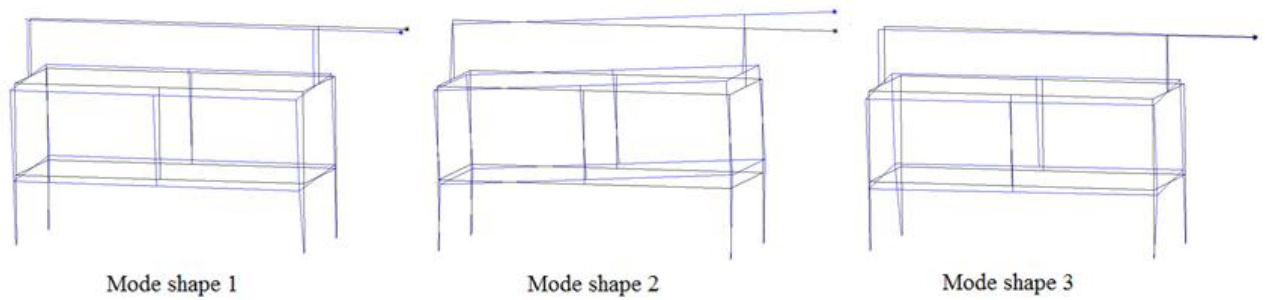


Figure 4.7: Three first mode shapes for the combined system. The bearing stiffness of the rotor-springs is very low. $k = 10^3 \text{ N/m}$

The mode shapes shows that the rotating disk is moving in a wobbling motion. The natural frequency analysis is performed in rotor speed interval between 0-1400 rpm, as shown in Figure 4.8. The LGW files can be found on the attached CD [LGW_8] and the Matlab plotting routine [Matlab_4].

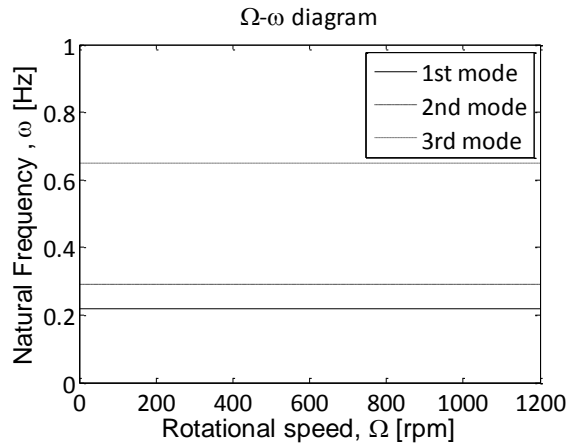


Figure 4.8: Ω - ω diagram for the combined system on very soft springs, $k = 10^3 \text{ N/m}$.

It is concluded, from Figure 4.8, that the natural frequencies of the combined system are unaffected of the gyroscopic effect. It is attempted to increase the diameter on the rotating disk by a factor of 100 but even that does not provoke any gyroscopic effect.

Another example, see Figure 4.9, where the overhang rotor is placed upon a flexible frame structure, has been analyzed but the conclusion is same as previous; the gyroscopic effect does not affect the natural frequency of the combined system.

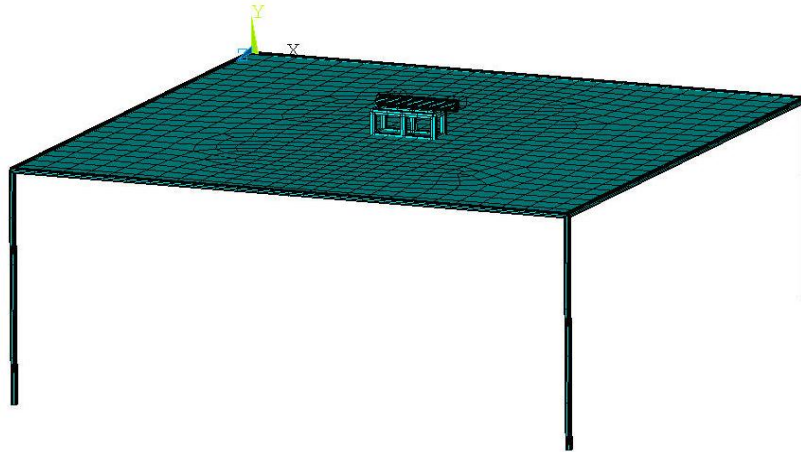


Figure 4.9: A combined system that consists of overhang rotor configuration supported a relative flexible frame structure.

4.5 Summary

A natural frequency analysis has been performed in Ansys and compared with an analytical solution

and identical results have been obtained. Thus, it can be concluded that the implementation of the gyroscopic effects in Ansys is correct. The solution procedure for a natural frequency analysis has been explained in detail.

A parameter study of an overhang rotor configuration has been performed and it has been demonstrated that the gyroscopic effect is most dominating for modes which involve a large wobbling motion, i.e. increasing the diameter of the disk or the shaft length result in an increased gyroscopic effect. Furthermore, a combined system has been analyzed and it is concluded that the gyroscopic effect does not affect the natural frequency of the combined system. Hence this lead to the following conclusion:

- It is important to include the gyroscopic effects in the analysis of the rotating rotors itself because the gyroscopic effect modifies the natural frequencies and the critical speeds.
- The gyroscopic effect is of minor influence when analyzing the natural frequencies of a combined system.

A transient analysis is performed in the following chapter and the steps involved are explained.

4.6 References

[4.1] Ansys Command Reference, Release 12.0, 2009. {412} and {1264}

[4.2] Rotordynamic Analysis Guide, Release 12.0, 2009. {25}

[4.3] <http://ecoperiodicals.com/2010/09/28/ge-boosts-energy-production-with-upgrades-of-2-5-mw-turbines>.

[4.1] and [4.2] can be found on the attached CD.

5 Transient Analysis

A transient analysis is performed in this chapter for the rotor configuration presented in chapter 3. The rotor is rotating and then simultaneously applied a rotation about a second axis which implies that the rotor basically behaves like a gyroscope, i.e. a movement is generated about the third axis. Moreover, the steps required to include the gyroscopic effect is explained and the essential commands are highlighted. The Ansys results are validated with an analytical solution. The latter is done to ensure that the contribution from the gyroscopic effect is correctly implemented in Ansys. The analytical solution is initially considered.

5.1 Defining the Motion

The rotor configuration, see Figure 5.1, is spinning with a constant angular velocity Ω , (1000 rpm) about the x -axis and is then simultaneous applied a rotation ω about the y -axis (1 degree pr. sec.).

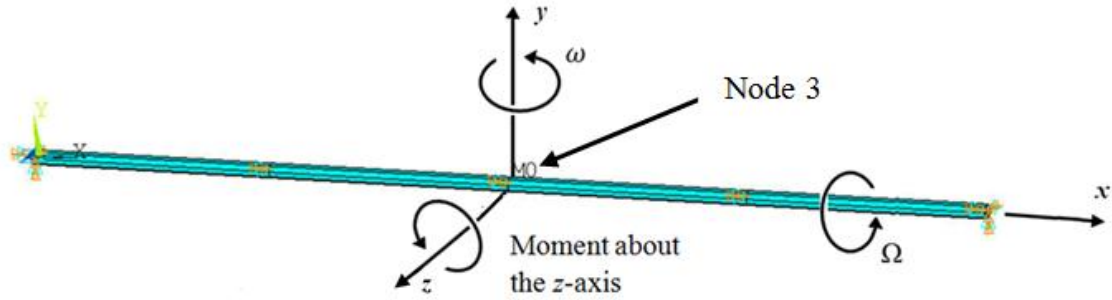


Figure 5.1: The rotor configuration is spinning with a constant angular velocity Ω . The disk is applied a rotational velocity ω , which is result in a gyroscopic bending moment about the z -axis.

This motion implies a change in the direction of the angular momentum $I_p \Omega$ which, due to the gyroscopic effect, results in a bending moment M_z about the z -axis. The bending moment M_z is determined from equation (1.4), derived in chapter 1.

$$M_z = I_p \Omega \omega, \quad (5.1)$$

where I_p is determined from $I_p = \frac{mD^2}{8}$. The diameter of the disk is 0.6 m, the thickness is 0.05 m and the density of the steel is 7800 kg/m^3 . Substituting these values into (5.1) one obtains a bending moment $M_z = 9.04 \text{ Nm}$. The system is solved in Ansys in the following section and the results are compared.

5.2 Transient Analysis in Ansys

There are basically three methods for conducting a transient analysis in Ansys (ANTYPE, TRANSIENT). These 3 methods are the full, reduced and modal Superposition methods [5.1].

The full method makes use of the full stiffness and mass matrices. The reduced method uses reduced matrices to calculate the harmonic solution. The superposition method sums mode shapes to calculate the harmonic response. The mode shapes are obtained from a modal analysis. The full method is simple and relative easy to use compared to the two other methods but is more costly in CPU time. The Full method is used in this thesis work. A transient analysis consists of the following steps:

1. Build the model - preprocessor. This is explained in chapter 3.
2. Apply the load – load history curve.
3. Establish Initial conditions.
4. Set the Solution Controls.
5. Solve the transient analysis.

5.2.1 Apply the load – Load History Curve

A Transient analysis, also called a time history analysis, involves per definition time-dependent loads. Loads are applied in load steps. The load is applied as a displacement (rotational) about the y-axis in node 3, as shown in Figure 5.1. The load (1 degree pr. sec) is defined with the following function

$$F(t) = \frac{1 \text{ degree}}{\frac{360}{(2\pi)}} \cdot \{Time\} = 0.01745 \text{ rad} \cdot \{Time\}, \quad (5.2)$$

which result in a constant angular velocity (0.01745 rad/s), as shown in Figure 5.2. The size of the time step is 1/10 sec. and the system is analyzed in the time interval 0-50 sec. The load is applied as a stepped function with the KBC,1 command. By doing this we subject the beam to loads at t=0.1 s., t=0.2 s. ... t=50 s.

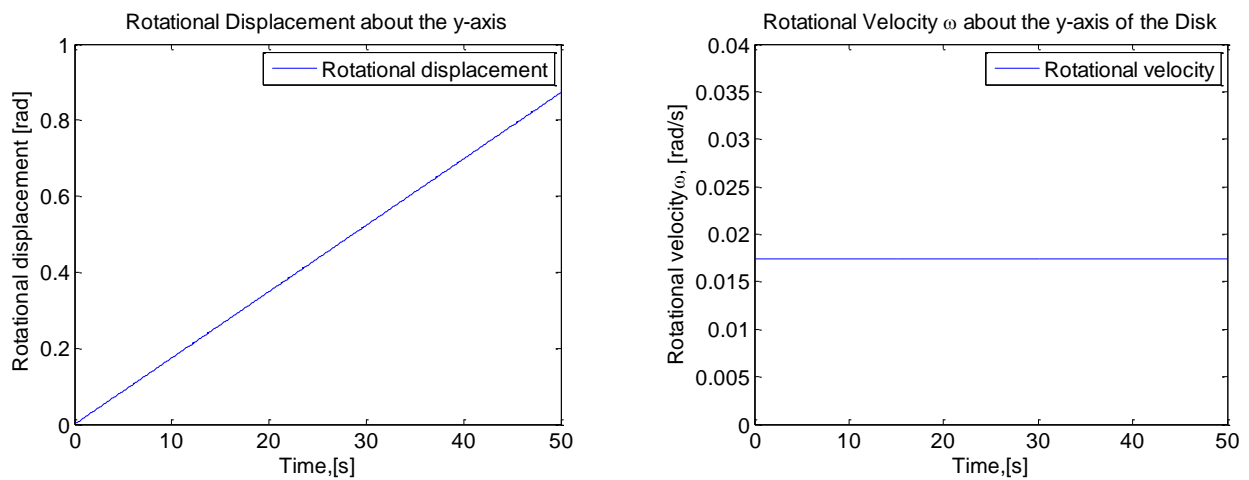


Figure 5.2: Left: Rotational displacement [rad] about the y-axis (node 3). Right: Rotational velocity ω [rad/s] about the y-axis (node 3).

5.2.2 Initial Conditions

The governing equation of motion is of second order. As a result, two set of initial conditions are required (both of these are by default set to zero in Ansys); initial displacement and initial velocity.

Wrong initial conditions can cause major a disturbance in the first part of the analysis. The rotor configuration has been assigned two set of initial condition in two separate analyses; Case one, no initial conditions (both values 0), illustrated with blue in Figure 5.3. Case two, initial displacement zero and initial velocity equal 0.01745 rad/s, illustrated with red in Figure 5.3. The results oscillates about the analytical solution, see Figure 5.3 (b), ($M_z = 9.04$ Nm) for both cases. However, this shows the importance of correct initial conditions. Moreover, it is concluded that the implementation of the gyroscopic effect is correct.

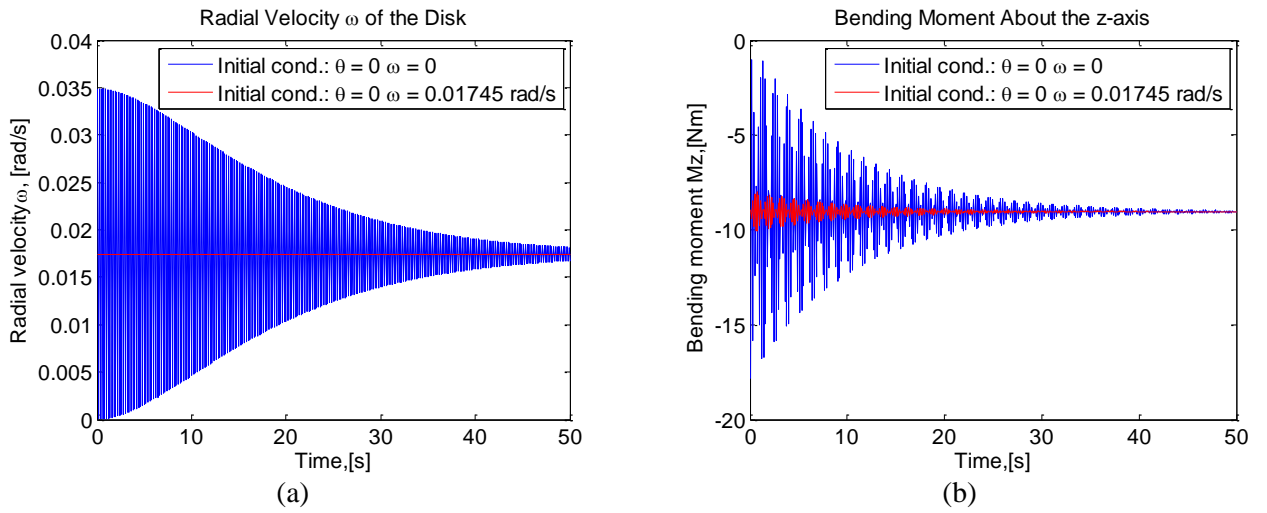


Figure 5.3 (a) Rotational velocity ω about the y-axis (node 3). (b): Bending moment about the z-axis (node 3).

The solution procedure is described in the following section.

5.2.3 Solution Controls

The gyroscopic effect is included by executing the command 'CORIOLIS,on,,on'. The gyroscopic moment M_z is zero if this command is not activated. It is not possible to include large-deflection effects because the gyroscopic matrix does not support large-deflection effects [5.2]. The large-deflection effect is de-activated with the "NLGEOM, OFF" command. The rotational velocity is defined using the CMOMEGA command. The CMOMEGA command recognizes all rotating part provided that these are grouped into one component. This is done with the CM command.

An implicit Newmark time integration scheme ($\beta = 0.25$, $\gamma = 0.5$) is used to determine the dynamic response. The solution procedure is given in the script below. The complete LGW file can be found on the attached CD [LGW_9] and the Matlab plotting routine [Matlab_5].

Code:

```
! ** Transient analysis
/solu
ANTYPE,TRANSIENT           ! Transient analysis
CORIOLIS,on,,on            ! Includes the Coriolis force in a stationary reference frame
NLGEOM, OFF                ! Large-deflection effects off
pi=acos(-1)                ! Defines pi
spn=1000*2*pi/60            ! Defines the rotation speed in rad/s
CMOMGA,shaft,spn,,,0,0,2,0,0 ! Specifies the rotational velocity of an element component
                              (shaft) about a user-defined rotational axis (x-axis)
time,50                    ! Defines the time at the end of the load step
deltime,0.1                ! Specifies the time load step size for this load step
kbc,1                      ! Stepped loading
outres,all,all             ! Write all results
solve                      ! Solve the system
```

5.3 Summary

It has been demonstrated that it is possible to include the gyroscopic effect in a transient analysis and that the initial conditions are of great importance. Furthermore, it has been explained how to perform a transient analysis with the gyroscopic effect included. The gyroscopic effect is included with the Coriolis command.

5.4 References

[5.1] http://www.ansys.stuba.sk/html/guide_55/g-str/GSTR5.htm

[5.2] http://www.kxcad.net/ansys/ANSYS/ansyshelp/Hlp_C_NLGEOM.html

6 Analysis of a Floating Wind Turbine

The modeling techniques described in the previous chapter are applied here in a practical example. A floating wind turbine is considered and the influence of gyroscopic effects is analyzed. This is done by comparing two situations where in the first situation the wind turbine is analyzed in parked condition (no rotation) and in the second in operational mode, i.e. the rotor (hub + blades) rotates.

A 5 MW wind turbine designed by NREL is used as a reference wind turbine. Detailed specifications of the tower, rotor (hub + blades) and nacelle are available in [6.1]. The NREL wind turbine was originally analyzed by Jonkman et al [6.1] in a program called FAST (Fatigue, Aerodynamics, Structures and Turbulence). A natural frequency analysis is performed in Ansys and the eigenfrequencies is compared to eigenfrequencies obtained in FAST in [6.1]. This is done to ensure that tower, rotor and nacelle properties are correct implemented in the Ansys model.

The buoyancy and stability of the wind turbine is not considered and the motion of the wind turbine due to hydrodynamic and wind load is simplified as a harmonic motion of wind turbine.

6.1 Generation of the Wind Turbine Model

The tower, rotor and nacelle properties, for the 5 MW wind turbine, is implement in an Ansys beam model in the following section. The tower is initially considered. Next, we define the support structure and finally the hub, rotor and nacelle are modeled.

6.1.1 Modeling of Tower

The tower properties of the NREL 5-MW wind turbine are given in Table 6-1. The modulus of elasticity is 210 GPa and the density of steel is $7,800 \text{ kg/m}^3$

NREL 5-MW reference	
Tower height	90 m
Tower base radius	3 m
Tower top radius	1.93 m
Tower thickness	0.027 m
Structural damping ratio	1 %

Table 6-1: Tower properties for the 5-MW reference wind turbine [6.1].

The tower is modeled with nine 3D beam elements, BEAM188 [6.6] . Each beam element represents a 10 m tower section and is, as shown in Figure 6.1, modeled with an average value of the respective tower section. The beam elements are numbered consecutively from the base of the tower, i.e. the first element is denoted 1, and the next element is denoted 2 and so on.

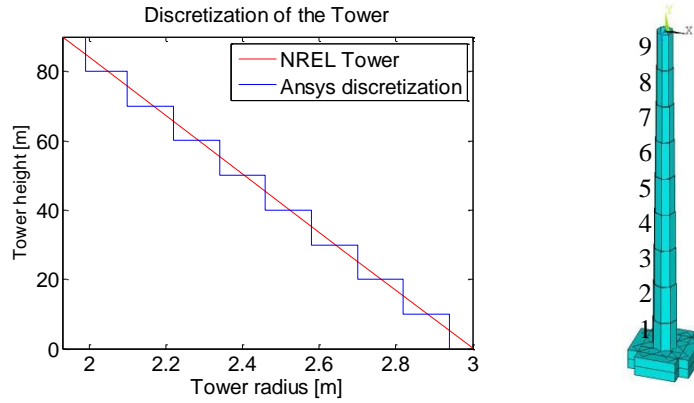


Figure 6.1 Left: Tower discretization in Ansys. Right: Ansys plot of the tower and the support structure.

6.1.2 Modeling of the Support Structure

The wind turbines tower is connected to a frame structure. A fluctuating load is applied to this support structure to simulate wave motion of a real ‘floating’ wind turbine. The fluctuating load is archived by applying a harmonic motion to each corner of the support structure. The harmonic motion is applied in the y -direction, as shown in Figure 6.2. This motion implies a rotation of the wind turbine about the z -axis which in combination with the angular momentum about the x -axis generates a gyroscopic torque in the tower (moment about the y -axis).

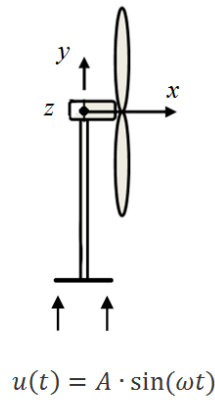


Figure 6.2 Harmonic rocking motion defined by $u(t) = A \cdot \sin(\omega t)$, where A is the amplitude and ω is the frequency of the motion.

The torque generated in the tower, due to the gyroscopic effect, result in a yaw motion of the support structure. This rotation implies an interaction between the water and the support structure which is simplified with spring elements, COMBIN14, placed in each corner of the support structure, as shown in Figure 6.3. The COMBIN14 [6.7] element is a uniaxial tension-compression element.

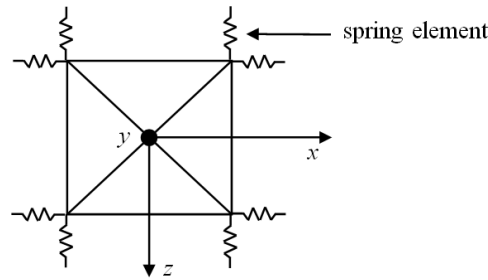


Figure 6.3 Illustration of the spring elements attached to each corner of the support structure.

A parameter study is performed in appendix E, page 67, where the dynamic response of the tower is analyzed, including the bending moment M_z , the gyroscopic torque T and the bending moment M_x , for different values of the spring stiffness. The spring stiffness is analyzed in the interval $k = 10^4 - 10^{12}$ kN/m. The bending moment M_z and the gyroscopic torque T is unaffected of the spring stiffness. The bending moment M_x is increased with a factor 2 for $k = 10^6$ N/m compared to $k = 10^{12}$ N/m. The spring stiffness $k = 10^6$ N/m is used in all analysis.

Lowering the spring stiffness result in an increased rotation of the support structure which result in an increased transverse shear force F_z . This explains why the bending moment M_x is increased when the spring stiffness is decreased.

6.1.3 Defining the Amplitude and Frequency of the Support Motion

The harmonic motion is defined as $u(t) = A \cdot \sin(\omega t)$, where A is the amplitude of the motion [m] and ω [rad/s] is the wave frequency. The models are analyzed with a 0.26 m amplitude. This motion corresponds to a 3 degree rotation of the wind turbine tower. Povl-Otto Nielsen [6.2] presents five wave heights and wave frequencies used for standard tests of wave energy machines. An average value of the wave frequencies is selected. As a result, a the wave frequency is 0.16 Hz, which corresponds to a wave period $T_{mean} = 6$ s.

6.1.4 Modeling of Hub, Rotor and Nacelle

The rotor and nacelle properties of the NREL 5-MW wind turbine are given in Table 6.2.

NREL 5-MW reference	
Rotor mass (hub + blades)	110000 kg
Distance from CM rotor to yaw axis	5.02 m
Nacelle mass	240000 kg
Distance from CM nacelle to yaw axis	1.9 m
Polar mass moment of inertia (hub+blades)	47104188 kg m ²

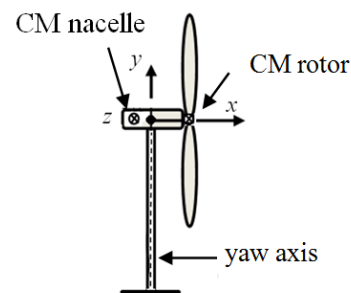


Table 6-2 Hub, blades and nacelle properties for the 5-MW reference wind turbine. CM is an abbreviation for Center Mass.

The rotor center mass (CM) is located 5.02 m from the yaw axis. The nacelle mass is located 1.9 m from the yaw axis. The shaft is modeled with 3D beam elements, BEAM188. Rotor and nacelle properties are modeled with mass elements, MASS21. This element type requires six real constant input values, a mass in the x , y and z -direction and a mass moment of inertia in the x , y and z -direction. The geometry of the complete model is divided into two separate parts. The first part consists of all rotating elements (shaft + rotor), as shown in Figure 6.4 (cyan). The second part consists of all non-rotating part (magenta). The rotor is connected to the non-rotating parts with bearings. Bearings can be visualized as very stiff springs. Bearings and the different spring elements available in Ansys is further described in appendix D. The rotor configuration is connected to the tower structure with two spring elements, as shown in Figure 6.4, with stiffness properties in the x , y and the z direction.

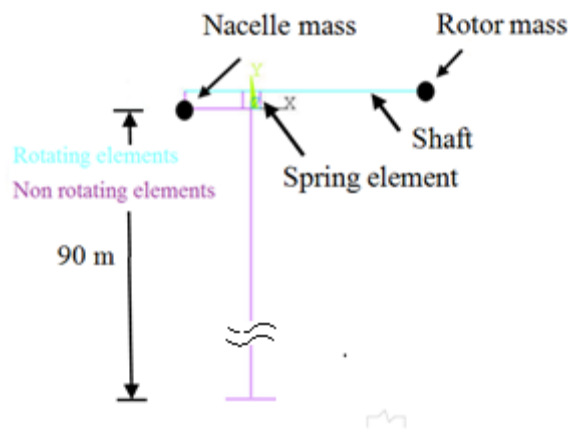


Figure 6.4: Ansys discretization. The cyan part is rotating and the magenta part is not rotating. The rotating and non-rotating parts are connected with infinitely stiff springs.

A natural frequency analysis is performed in the following section and the Ansys eigenfrequencies are compared with FAST natural frequencies given in [6.1]. This is done to ensure that tower, rotor and nacelle properties are correctly implemented in the Ansys model.

6.2 Natural Frequency Analysis

The solution procedure, described in Chapter 4, is used to implement the gyroscopic effect in the natural frequency analysis. The first three natural frequencies from the natural frequency analysis is

plotted in a Ω - ω diagram, where Ω is the rotational speed of the rotor and ω is the natural frequency, see Figure 6.5. The NREL natural frequencies are given as constant values in [6.1] but plotted as straight lines to be able to compare them with the Ansys natural frequencies.

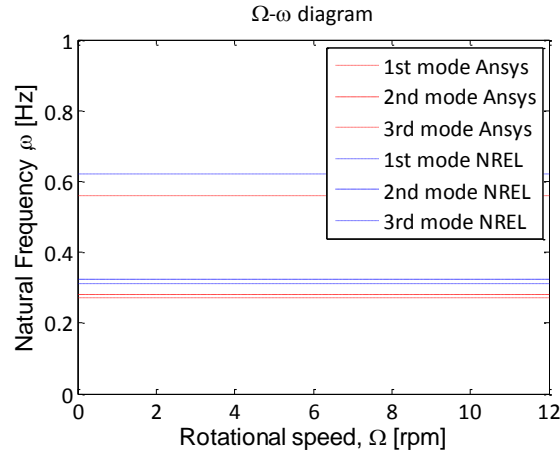


Figure 6.5 diagram for the NREL and Ansys solution.

The Ansys natural frequencies are, as shown in Figure 6.5, completely straight lines. Hence, it is concluded that the natural frequencies are unaffected by the gyroscopic effect. Furthermore, the natural frequencies determined in Ansys are in agreement with FAST results (less than 10 percent difference), i.e. the tower, rotor and nacelle properties are considered to be correctly implemented in Ansys.

6.3 Transient Analysis of the Wind Turbine

Three different models shown in Figure 6.6 are considered in a transient analysis in the following sections. In the first model we apply a rocking motion to the support structure, illustrated with arrows in Figure 6.6, and the rotor is analyzed in a parked mode, i.e. the rotor does not rotate. In the second model we analyze the system where the rotor rotates and the influence of the gyroscopic effect is analyzed. However, the second model is a simplification of a real rotor configuration because rotor unbalances are neglected. The third model includes a rotor unbalance. The wind turbine rotates with 12 rpm in model 2 and 3. The LGW files can be found on the attached CD [LGW_10] (model 1), [LGW_11] (model 2) and [LGW_12] (model 3) and the Matlab plotting routine [Matlab_6].

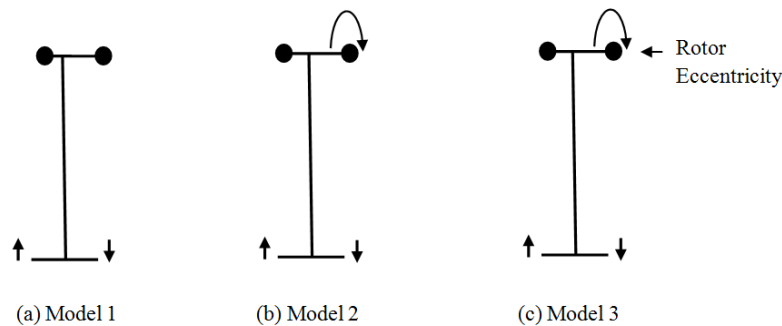


Figure 6.6 A rocking motion is applied to the support structure of all models. Model 1: The rotor is not rotating. Model 2: The rotor is rotating. Model 3: The rotor is rotating and an eccentricity is applied.

Model 3 includes a rotor unbalance, which results in an unbalanced force $F = m\varepsilon\Omega^2$, where m is unbalance mass, ε is the eccentricity and Ω is radial rotational speed of the rotor (rad/s). It is assumed that the unbalanced mass is 5 kg, which is the maximum mass difference that can be allowed between two blades. This unbalance is assumed to be located in blade center mass (20.475 m) [6.1]. The amplitude and frequency of support motion is presented in the following section.

6.3.1 Solution Controls

An implicit Newmark time integration scheme ($\beta = 0.25$, $\gamma = 0.5$) is used to determine the dynamic response. It is recommended [6.3] to choose a time step size according to $1/20f$, where f is the highest frequency of interest or alternatively choose a value which is small enough to follow the load function. The load frequency is 0.16 Hz and since the dynamic response is expected to be dominated by the lowest mode shape 0.28 Hz we obtain a recommended minimum iteration time step 0.17 s. Thus, we use a time iteration step of 1/10 sec. The system is analyzed in the time interval 0-400 sec.

6.3.2 Damping

Jonkman et al [6.1] use a structural-damping ratio of 1 % of critical in all modes in the NREL study.

It is not possible to define a constant damping ratio for each frequency in full transient analysis in Ansys [6.4]. Instead, we use a stiffness weighted damping [6.5]

$$[C] = \beta[K], \quad (6.1)$$

where β is defined from

$$\beta = \frac{2\xi}{\omega}, \quad (6.2)$$

where ω is the frequency of the most dominating frequency and ξ is the damping ratio. It is assumed that the dominating frequency is the lowest frequency 0.28 Hz. As a result, the β value is determined to 0.011. This β should not be confused with the integration parameter β .

6.3.3 Verification of the method to apply the load

A transient analysis has been performed for a simple system, see Figure 6.7 (a). The system is applied a harmonic base motion, $u(t) = \sin(\omega t)$, and a harmonic force $F(t) = \cos(\omega t)$. The system is analyzed in Ansys and verified with an analytical solution. This is done to ensure that the harmonic motion is applied correctly in Ansys. The solution procedure and the mass and stiffness properties are described in Appendix F. The analytical result is similar to the Ansys re-

sult, see Figure 6.7 (b), i.e. it must be concluded that we are able to apply the harmonic displacement- and force correctly in Ansys.

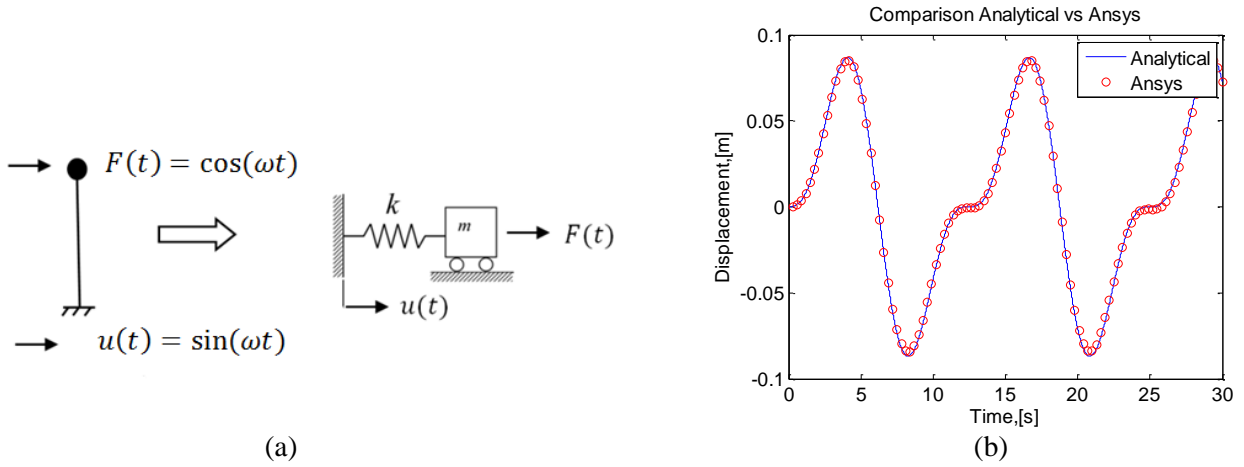


Figure 6.7 (a) Simple mass spring system. (b) Time response of the displacement of the mass for the analytical and Ansys solution.

6.3.4 Defining the Failure Criteria for the Tower

The element type BEAM188 used to model the tower has six degrees of freedom in each node. As a result, the following forces, see Figure 6.8, are obtained; axial force N , torque T about the y -axis, bending moment M_x about the x -axis, bending moment M_z about the z -axis, transverse shear force F_x and a transverse shear force F_z .

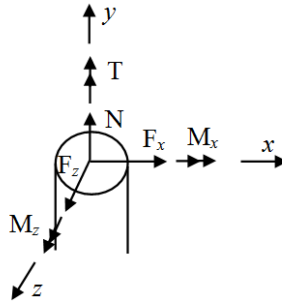


Figure 6.8 Reaction forces for the 3D beam element in Ansys.

Model 1-3 is compared to each other by using Von Mises failure criteria in two locations of the cross-section in terms of the stress components, given by

$$\sqrt{\sigma_y^2 + 3\tau_{yx}^2 + 3\tau_T^2} \geq f_y, \quad (6.3)$$

where σ_y , τ_{yx} and τ_T are given by

$$\begin{aligned} \sigma_{y1} &= \frac{N}{A} + \frac{M_z}{I_z} \cdot \frac{D}{2}, & \tau_{yx1} &= \frac{F_z}{A_s}, & \tau_T &= \frac{T}{I_p} \cdot \frac{D}{2}, \\ \sigma_{y2} &= \frac{N}{A} + \frac{M_x}{I_x} \cdot \frac{D}{2}, & \tau_{yx2} &= \frac{F_x}{A_s}, \end{aligned} \quad (6.4)$$

where σ_{y1} and τ_{yx1} refers to point 1, see Figure 6.9, and σ_{y2} and τ_{yx2} refers to point 2. A is the cross section area, $A_s = \frac{A}{2}$, I_z and I_x are the second moment of inertia, D is the diameter of the tower and I_p is the polar mass moment of inertia. The first point is influenced by the bending moment M_z , the normal force N , the transverse shear force F_z and the gyroscopic torque T . The second point is influenced by the bending moment M_x , the normal force N , the transverse shear force F_x and the gyroscopic torque T .

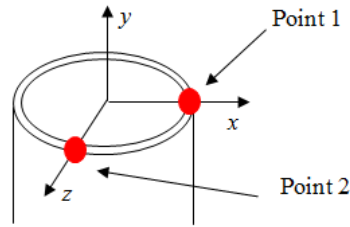


Figure 6.9 Definition of the points 1 and 2

The Von Mises stress is compared in the two points defined in Figure 6.9 in the bottom of the tower and in the top of the tower, node 1 and node 10, respectively. The node numbering is given in Figure 6.10. Displacements are compared in node 2 and 10.

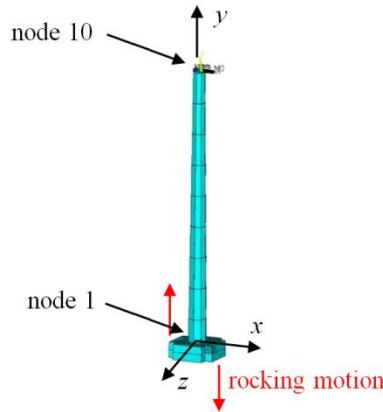


Figure 6.10 Node numbering for the wind turbine tower.

6.4 Results of the Transient Analysis

6.4.1 Analysis of the Displacements Model 1

Initially, the deflection of the tower, due to the harmonic motion, is analyzed. Two analyses have been performed. Firstly, an analysis of the complete wind turbine. Secondly, an analysis of a reduced model where the nacelle and rotor mass is removed. Figure 6.11 (a) shows the tower deflection in the x -direction for the complete model (red), the reduced model (blue) and finally a rigid movement (black) of the tower due to the harmonic motion, defined in section 6.1.3. The harmonic motion equals a 3 degree rotation of the tower, which gives a 4.71 m rigid movement of the top node (node 10). Figure 6.11 (b) shows the time history of the displacement in the x -direction for node 2 and 10 for the complete model.

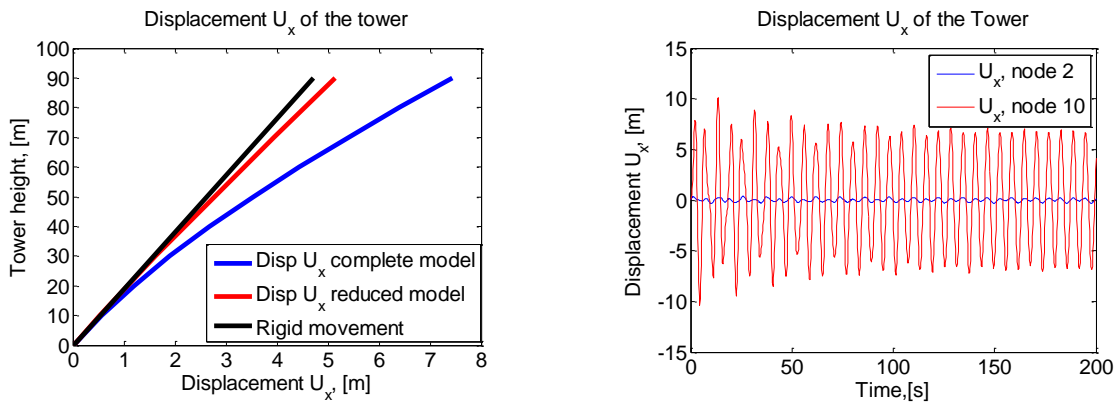


Figure 6.11 Left: Deflection of the tower at time=128.4 s. Right: Time history of U_x at node 2 and 10 for the complete model.

The complete model is displaced 7.43 m in the top node. This deflection is a combination of a 4.71 m rigid movement and a 2.72 m deflection in the tower. The tower deflection is reduced to 0.433 m for the reduced model, i.e. the nacelle and rotor mass increase the tower deflection with a factor 6.3.

6.4.2 Relation between the Load Function and the Response model 1

Model 1 is analyzed with two different load functions and it is examined if there is a linear relation between the load and the response. A linear relationship implies that we can predict the value of the displacements and section forces to any other load functions. A ratio is determined between two different load functions, where the amplitude of the later is twice as large as the first. The ratio is 1 if there is a linear relationship between the load and the response.

$$ratio = \frac{U_{x \text{ large amplitude}}}{2 \cdot U_{x \text{ small amplitude}}} \quad (6.5)$$

The ratio, see Figure 6.12 , is calculated for all the nodes along the tower at the time instant 128.4 s.

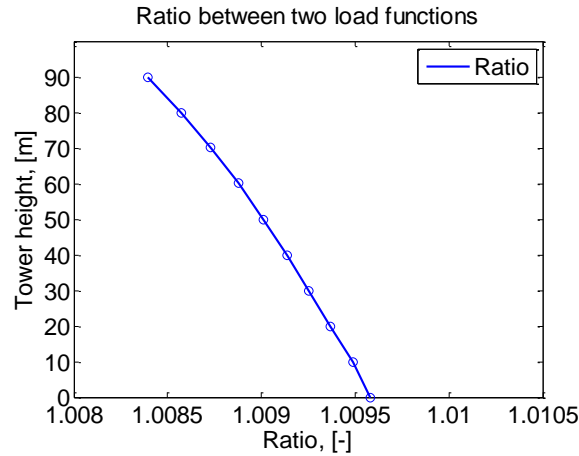


Figure 6.12 Ratio between responses for two different load functions

Figure 6.12 shows that the ratio is between 1.0085 and 1.0095. As a result it is concluded that there is a linear relationship between the load and the response.

6.4.3 Comparison of Section Forces model 1 and model 2

The section forces is analyzed and compared for model 1 and model 2 in the following section. The main difference between model 1 and model 2 is that the rotation of the rotor introduces a gyroscopic torque T in the tower. The gyroscopic torque is constant along the tower. This is illustrated in Figure 6.13 where the time history of the gyroscopic torque is plotted in node 1 and node 10 for model 2.

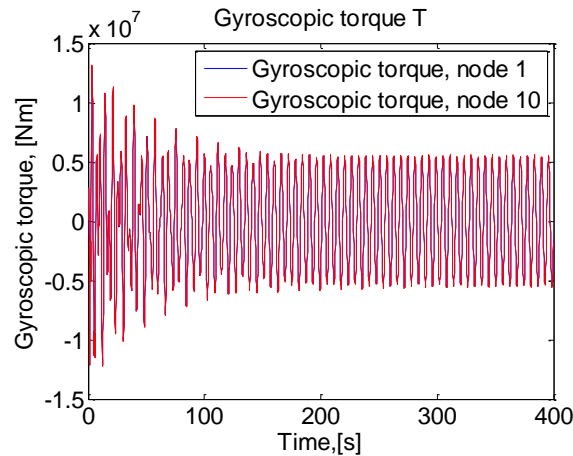


Figure 6.13 Gyroscopic torque in the tower in node 1 and node 10.

The torsion stress, due to the gyroscopic torque, is 9.80 MPa in the top section of the tower and 4.07 MPa in the bottom section of the tower. The gyroscopic torque T is small compared to the bending moment M_z . The bending moment M_z is relative large because of the tower deflection,

described in 6.4.1. The magnitude of T is $1/60$ of M_z . The gyroscopic torque T generates a small torsion in tower, see Appendix G for results, which rotates the nacelle-, hub and rotor mass about the y -axis. The principle is illustrated in Figure 6.14 (magnified to illustrate point).

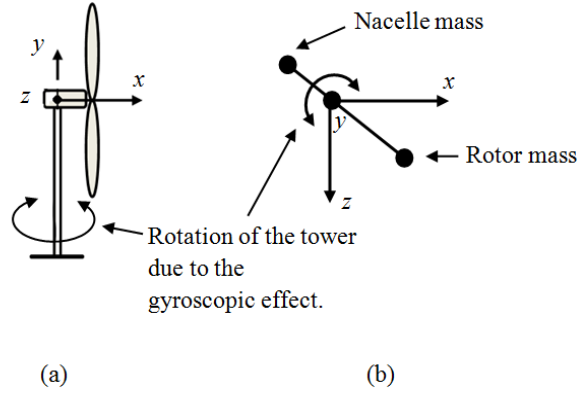


Figure 6.14 (a) Side view of the wind turbine. (b) Top view of the wind turbine. The gyroscopic torque T introduces a shear force F_z and a bending moment M_x .

The torsion (rotation) of the tower introduces a transverse shear force F_z and a bending moment M_x . The magnitude of F_z is small compared to F_x . The relation between F_z and F_x is about $1/100$.

In summary, the difference between model 1 and model 2 is the presence of a gyroscopic torque T , a shear force F_z and a bending moment M_x in the model which includes the rotation of the rotor (model 2). The time-history of the section forces are shown in Figure 6.15 for model 1 and model 2, in the bottom of the tower (node 1).

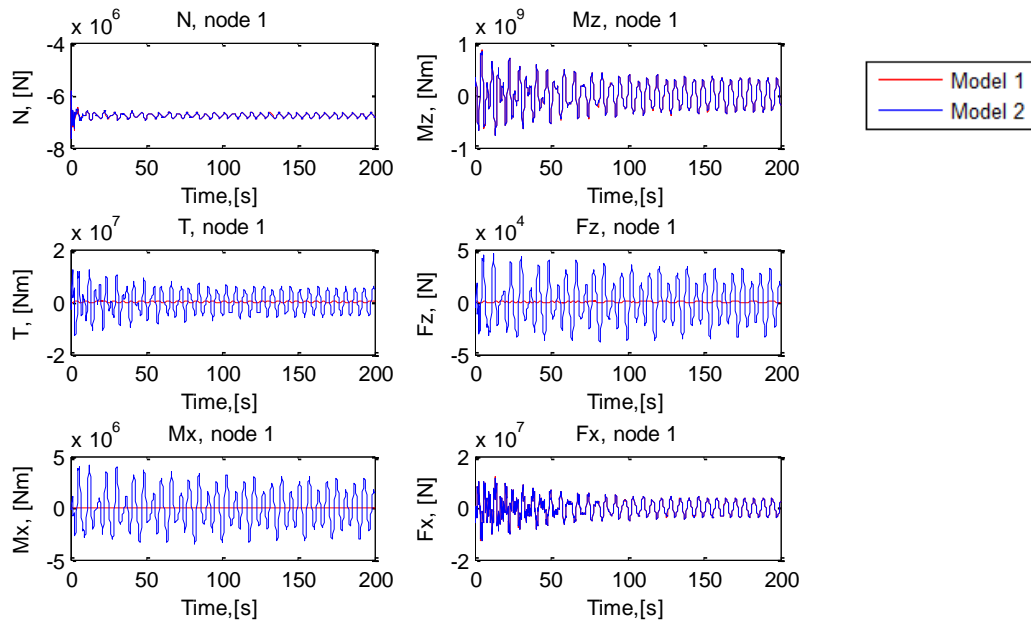


Figure 6.15 Section forces model 1 and model 2 in node 1.

The time-history of the section forces are shown in Figure 6.16 for model 1 and model 2 in node 10.

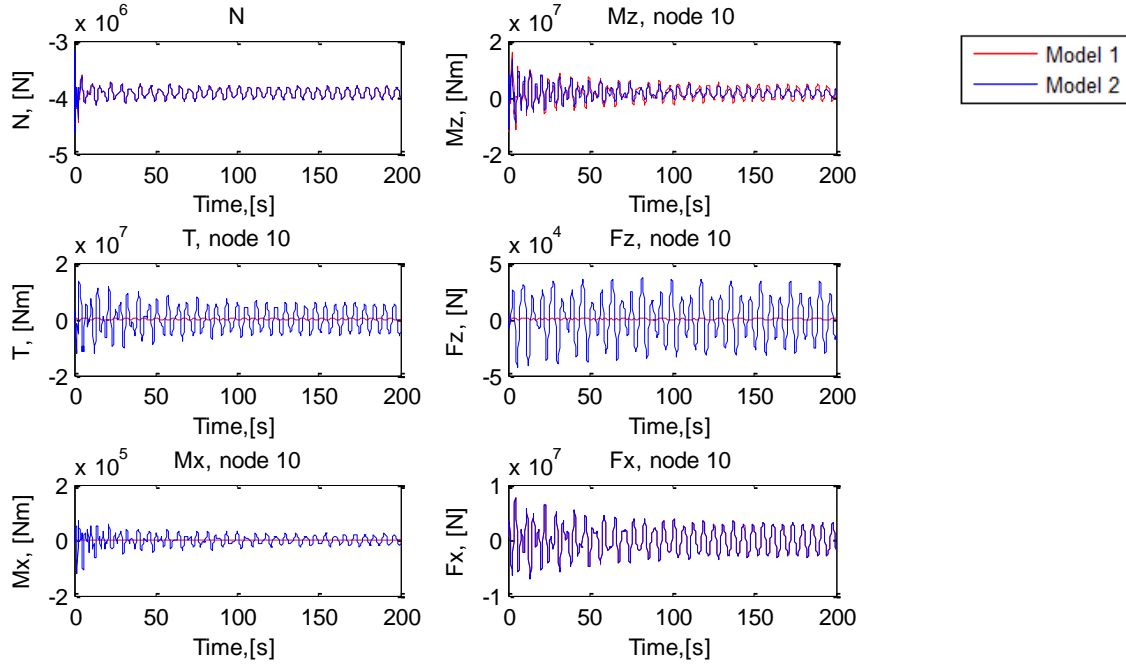


Figure 6.16 Section forces in node 10 for model 1 and model 2.

Figure 6.15 shows that the normal force N , the bending moment M_z and the transverse shear force F_x is similar in for model 1 and model 2 in node 1. A gyroscopic torque T , a shear force F_z and a bending moment M_x is, as explained previously, introduced due to the gyroscopic effect.

Figure 6.16 shows that the normal force N , the transverse shear force F_x is similar in for model 1 and model 2 in node 10. The bending moment M_z is about 15 percent smaller for model 2 compared to model 1. The displacement is the same for model 1 and model 2. These results are presented in appendix G. The rotation about the z -axis is 1 percent smaller for model 2 compared to model. These results are also presented in appendix G.

The section forces vary with time. We will in the following section examine the relation between the section forces at a certain time.

6.4.4 Analysis of the Relation between the Section Forces to a Certain Time

It was shown in the previous section that the gyroscopic effect introduces additional forces into the system. The section forces does not reach a maximum value at the same time. The maximum magnitude of the bending moment M_z and the transverse shear force F_x is observed when the tower deflection is maximum. Moreover, the gyroscopic torque T , the transverse shear force F_z and bending moment M_x is zero at this time. The principle is illustrated in Figure 6.17.

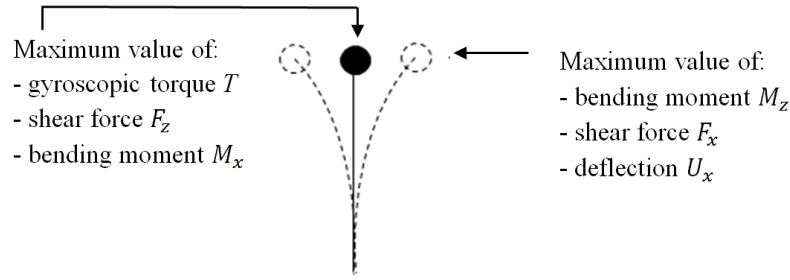


Figure 6.17 Principle sketch of when the section forces are maximum in the tower.

The time history of the section forces are shown in Figure 6.18 in the time interval $t = 154 - 174$ s. Note that the displacement U_x (top left), the bending moment M_z (top middle) and the shear force (bottom middle) are maximum when the gyroscopic torque T , the shear force F_z and a bending moment M_x is zero.

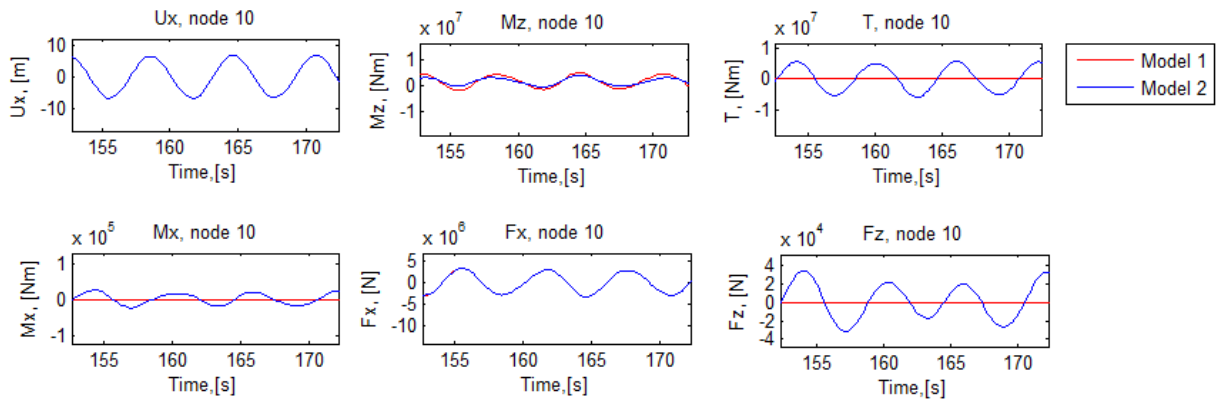


Figure 6.18 Section forces in the interval $t = 154 - 174$ s

As a result, The Von Mises stress is generated from a contribution from N , M_z and F_x when the tower deflection is maximum and a contribution from N , M_x and F_z and T when the tower deflection is zero. Point 1, see Figure 6.19, is affected by N and M_z when the tower deflection is maximum and N , F_z and T when the deflection is zero.

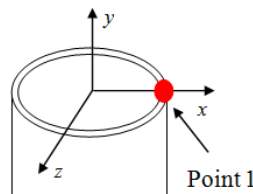


Figure 6.19 Illustration of point 1.

Point 2, see Figure 6.20, is affected by N and F_x when the tower deflection is maximum and N , M_x and T when the deflection is zero.

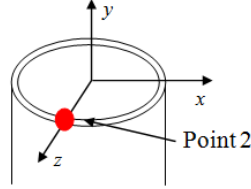


Figure 6.20 Illustration of point 2.

Recall from the previous section that the magnitude of T is about 1/60 of M_z and the relation between F_z and F_x is about 1/100. This means M_z and F_x dictates the maximum value of the Von Mises stress in point 1 and point 2. As a result, the contribution from T , F_z and M_x will only affect the minimum value of the Von Mises stress.

6.4.5 Von Mises Stress Model 1 and Model 2 in the Bottom of the Tower (node 1)

Figure 6.21 (a) shows the Von Mises stress history in the bottom of the tower (node 1) in point 1. The gyroscopic effect gives a contribution from F_z and T when M_z is zero. However, the contribution is very small (less than 0.1 percent) and cannot be seen on the Figure 6.21.

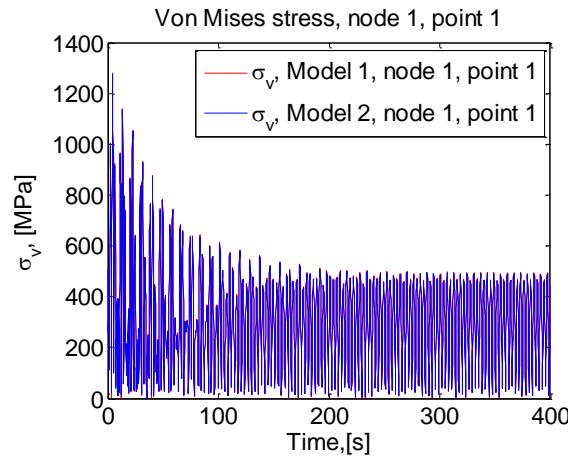


Figure 6.21: Von Mises stress for model 1 and model 2 in node 1, point 1

Figure 6.22 shows the Von Mises stress history in the bottom of the tower (node 1) in point 2. The gyroscopic effect introduces, as explained in the previous section, a bending moment M_x and a gyroscopic torque T when the tower deflection is zero, i.e. when the dominating contribution from the shear force F_x is zero. This contribution affects the lower value of the Von Mises stress as shown in Figure 6.22.

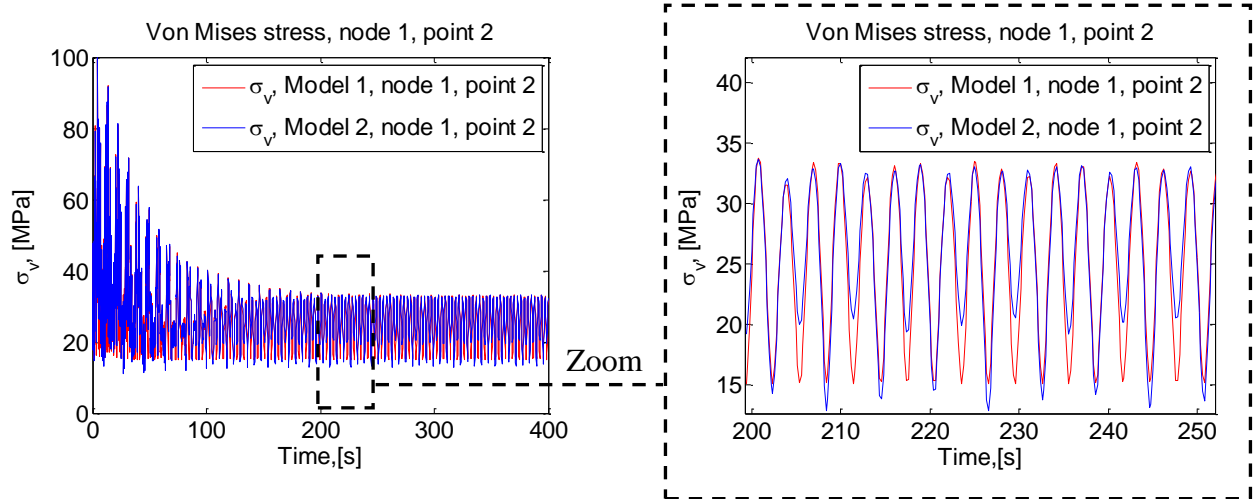


Figure 6.22: Von Mises stress for model 1 and model 2 in node 1, point 2.

6.4.6 Von Mises Stress Model 1 and Model 2 in the top of the Tower (node 10)

Next, we analyze the Mises stress in node 10. Figure 6.23 shows the Von Mises stress history in node 10 in point 1. The Von Mises stress is about 35 percent smaller for model 2 compared to model 1 in point 1. This difference is caused by the difference in the bending moment M_z .

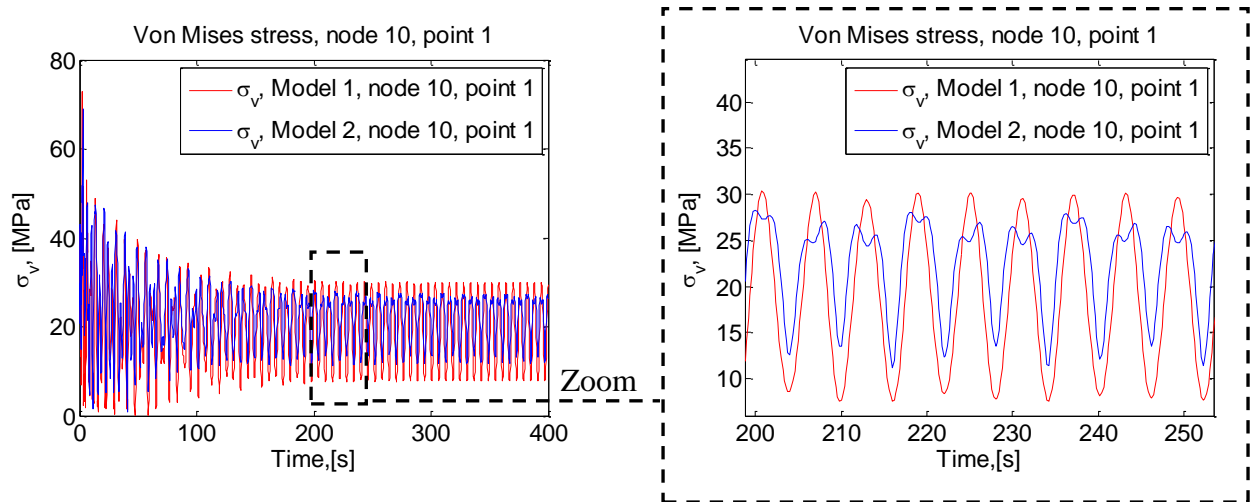


Figure 6.23: Von Mises stress for model 1 and model 2 in node 10, point 1.

Figure 6.24 shows the Von Mises stress history in the top of the tower (node 10) in point 2. The gyroscopic effect gives a contribution from F_z and T when F_x is zero which increases the minimum value of the Von Mises stress with 12 percent.

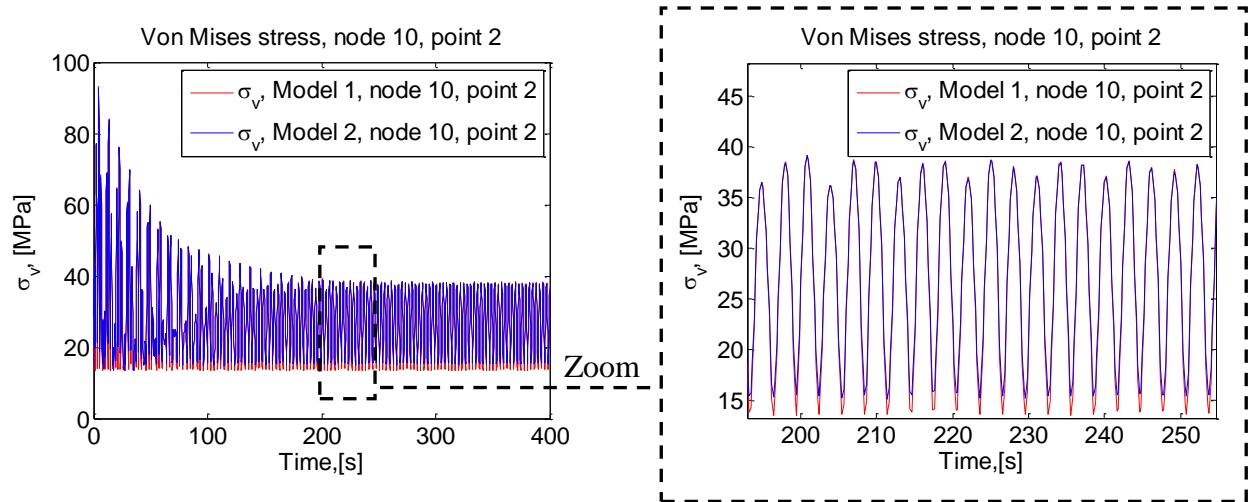


Figure 6.24 Von Mises stress for model 1 and model 2 in node 10, point 2.

6.4.7 Model 3

Model 3 includes a rotor unbalance force from an unbalance mass (5 kg) which rotates with a 20.475 m eccentricity. The dynamic response, including the displacements of the tower and the bending moments M_z and M_x , has been analyzed. The results obtained from model 3 are identical to the results obtained from model 2, i.e. the forces introduced due to the a 5 kg eccentric mass is negligible compared the bending moment generated when the wind turbine undergoes a harmonic motion.

6.5 Summary

The modeling techniques from chapter 3, 4 and 5 have been applied to a ‘floating’ wind turbine. A wind turbine designed by NREL has been used as a reference model. A natural frequency analysis has been used to verify that the tower, rotor and nacelle properties were correct implemented in the Ansys model. The influence of the gyroscopic effect has been examined by comparing the transient response of a model in parked condition and a model in operational mode. The findings of the analysis are:

- There is a linear relation between the load and the response.
- A gyroscopic torque is generated in the model which includes the rotational inertia of the rotor (model 2). This torque generates a small torsion in the tower which introduces two additional section forces, a shear force F_z and a bending moment M_x .
- The forces introduced due to the gyroscopic effect are very small compared to the forces generated due to the harmonic motion of wind turbine.
- A small decrease is observed in the bending moment M_z in the top tower section for model 2. The bending moment M_z is the same for the remaining tower sections because the shear force F_x is identical for model 1 and model 2.

- The maximum value of the Von Mises stress is unaffected of the gyroscopic effect in all sections of tower except the top section where it is reduced with 35 % due to the difference in the bending moment M_z .

Thus, it is concluded that the forces introduced due to the gyroscopic effect of the rotating rotor is of minor influence compared to the forces introduced due to the harmonic motion of the support structure.

6.6 Discussion of the Results and Methods

We will in the following section discuss the following:

1. Is the size of the amplitude of the harmonic motion realistic?
2. The comparison method based on Von Mises stress.
3. Is the findings in this thesis in agreement with previous research?

(1) The amplitude of the harmonic motion corresponds to a 3 degree rotation of the wind turbine which results in a 7.43 m displacement of the top of the tower (a combination of a rigid movement and a deflection in the tower). This displacement is very large and it can be discussed if the wind turbine can operate under these circumstances. In Addition, the maximum Von Mises stress observed is 500 MPa. This value is too large as well. As a result, it would have been more realistic to analyze the wind turbine with a smaller load function, i.e. the amplitude of the motion should have been smaller.

(2) The influence of the gyroscopic effects is examined by comparing the Von Mises stress for each model. It should be noted that this method does not give a fair picture of the influence of the gyroscopic effect because of a relative large contribution from the normal force (self-weight of the structure), i.e. analyzing the system with a very small harmonic motion does not give any difference in the Von Mises stress because of the dominating contribution from the normal force. This means that we cannot use the linear relation between the load and the response to predict the influence of gyroscopic effects for other load functions.

(3) It is very difficult to compare the results directly to previous research since the basis of the analysis including the models and loading conditions are different. However, it is possible to compare the tendencies. The tendencies observed in this thesis work are compared to work done by J.M.Jonkman et. al and X.Liu et al.

- J.M.Jonkman et. al [6.8] analyze an offshore wind turbine supported by a barge with catenary moorings in fully coupled Aero-Hydro-Servo-elastic simulation tool and presents the results of their work as a ratio between the loading of an offshore- and an onshore wind turbine.

- X.Liu et al [6.9] analyze an onshore wind turbine and examine the influence of gyroscopic effects by comparing a model with no rotation (parked) to a wind turbine with the rotation of the rotor included.

Both J.M.Jonkman et. al and X.Liu et al observe a gyroscopic torque in the tower due to the gyroscopic effect and they conclude independently that the gyroscopic torque in the tower generates a small torsion which increases the side-to-side displacement of the tower. These findings correspond to the findings in this thesis. J.M.Jonkman et. al does not comment on the importance of the gyroscopic effect. X.Liu et al finds an increase in the Von Mises stress which is less than 5 % and concludes that the gyroscopic effect can be ignored in the study of wind turbines. The last observation does not correspond to findings in this thesis because the maximum value of the Von Mises stress is unaffected by the gyroscopic effect.

6.7 References

[6.1] Jason Jonkman, Sandy Butterfield, Walt Musial, George Scott. Definition of a 5-MW Reference Wind Turbine for Offshore System Development.

[6.2] Povl-Otto Nielsen. Måling af bølgeenergi.

[6.3] http://www.kxcad.net/ansys/ANSYS/ansyshelp/Hlp_G_MULDAMPING.html

[6.4] http://www.kxcad.net/ansys/ANSYS/ansyshelp/Hlp_G_STR5_12.html

[6.5] C. Cai, H. Zheng, M. S. Khan and K. C. Hung. Modeling of Material Damping Properties in ANSYS. Defense Systems Division, Institute of High Performance Computing 89C Science Park Drive, Singapore Science Park I, Singapore 118261. {7}

[6.6] http://www.kxcad.net/ansys/ANSYS/ansyshelp/Hlp_E_BEAM188.html

[6.7] http://www.kxcad.net/ansys/ANSYS/ansyshelp/Hlp_E_COMBIN14.html

[6.8] J.M. Jonkman and M.L. Buhl, Jr. Loads Analysis of a Floating Offshore Wind Turbine Using Fully Coupled Simulation. *Conference Paper NREL/CP-500-41714 June 2007. {23}*

[6.9] X.Liu, K.R Leimbach and D. Hartmann. Investigation of the Gyroscopic Effect on a Wind Turbine Model with Ansys. Institute of Computing in Engineering, Ruhr-University of Bochum, Germany. Paper 147.

[6.1] , [6.2], [6.5], [6.8] and [6.9] can be found on the attached CD.

7 Conclusion

The primary objective of this thesis is to analyze a wind turbine supported on a rocking foundation and determine the importance and relevance of gyroscopic effects. Hence, this can only be achieved if we know how to include these effects into the numerical simulation tool (Ansys). The main conclusions of this thesis are:

1. It is not straightforward to perform an analysis in Ansys which includes gyroscopic effects. Firstly, because there is a limited number of examples/tutorials on this subject and secondly because there are some special commands which has to be activated before running the analysis, i.e. the effect does not come out naturally.
2. It is important to separate rotating and non-rotating part when building a model and apply the rotational velocity to the correct parts.
3. The gyroscopic effect is included with Coriolis command in Ansys.
4. The gyroscopic effect results in a non-symmetric damping matrix and requires a non-symmetric solver when performing a natural frequency analysis in Ansys.
5. Gyroscopic effects modify the natural frequencies and the critical speeds of rotating rotors but do not change the natural frequencies of a combined system (rotating part and a stationary part). Hence, it is important to include the gyroscopic effect when analyzing and designing the rotor itself but the effect is of minor influence when analyzing the natural frequencies of the combined system.
6. The damping has a major impact on the transient response of the wind turbine tower. In particular, if the dynamic loading is applied with wrong initial conditions or applied as an impact load.
7. The gyroscopic effects introduce a gyroscopic torque in the wind turbine tower which generates a small torsion. This torsion introduces additional section forces in the tower.
8. The maximum value of the Von Mises stress is unaffected of the gyroscopic torque and the additional section forces.
9. It is difficult to give a precise estimate of the exact influence of the gyroscopic effect because the Von Mises stress is affected by a relative large normal force from the self-weight of the wind turbine.
10. The tendencies observed in this thesis work correspond to previous research.

8 Overview of the Attached Disk

8.1 Ansys LGW files

[LGW_1] Modeling of geometry for the simple rotor configuration in chapter 3, section 3.2.

[LGW_2] Natural frequency analysis of the simple rotor configuration. The results are presented in chapter 4, section 4.3.

[LGW_3] Natural frequency analysis of the simple rotor configuration. Short rotor. The results are presented in chapter 4, section 4.4.2.

[LGW_4] Natural frequency analysis of the simple rotor configuration. Long rotor. The results are presented in chapter 4, section 4.4.2

[LGW_5] Natural frequency analysis of the simple rotor configuration. Nominal. The results are presented in chapter 4, section 4.4.3

[LGW_6] Natural frequency analysis of the simple rotor configuration. Heavier disk. The results are presented in chapter 4, section 4.4.3

[LGW_7] Natural frequency analysis of the simple rotor configuration. Large diameter. The results are presented in chapter 4, section 4.4.3

[LGW_8] Natural frequency analysis of a combined system. The results are presented in chapter 4, section 4.4.4.

[LGW_9] Transient analysis of a simple rotor configuration. The results are presented in chapter 5, section 5.2.2.

[LGW_10] Transient analysis of a model 1. The results are presented in chapter 6, section 6.4.

[LGW_11] Transient analysis of a model 2 The results are presented in chapter 6, section 6.4.

[LGW_12] Transient analysis of a model 3.

[LGW_13] Harmonic analysis of the simple rotor configuration. The results are presented in appendix G.

8.2 Matlab Plotting Routines

[Matlab_1] Plotting routine for the natural frequency analysis of the simple rotor configuration, [LGW_2]

[Matlab_2] Plotting routine for the natural frequency analysis of the simple rotor configuration with short and long shaft, [LGW_3] and [LGW_4]

[Matlab_3] Plotting routine for the natural frequency analysis of the simple rotor configuration with nominal mass, heavier disk and large diameter, [LGW_5] , [LGW_6] and , [LGW_7].

[Matlab_4] Plotting routine for the natural frequency analysis of the a combined system.,[LGW_8].

[Matlab_5] Plotting routine for the transient analysis of a simple rotor configuration, [LGW_9].

[Matlab_6] Post processing of the Ansys results in chapter 6.

[Matlab_7] Plotting routine for the harmonic analysis of the simple rotor configuration.

Appendix A

A.1 Derivation of the Stiffness Matrix

The displacement and rotation for a beam submitted a force F is given by [A.1]

$$\delta = \frac{FL^3}{3EI} = \alpha_1 F, \quad \theta = \frac{FL^2}{2EI} = \alpha_2 F. \quad \text{---} \downarrow F \quad (\text{A.1})$$

The displacement and rotation for a beam submitted to and end moment M is given by

$$\delta = \frac{ML^2}{EI} = \alpha_2 M, \quad \theta = \frac{ML}{EI} = \alpha_3 M. \quad \text{---} \curvearrowright M \quad (\text{A.2})$$

From there expressions, the displacement and rotation can be obtained by

$$u = \alpha_1 F_x + \alpha_2 M_y, \quad v = \alpha_1 F_y + \alpha_2 (-M_x), \quad (\text{A.3}) \text{ and } (\text{A.4})$$

$$-\theta = \alpha_2 F_y + \alpha_3 (-M_x), \quad \psi = \alpha_2 F_x + \alpha_3 M_y, \quad (\text{A.5}) \text{ and } (\text{A.6})$$

this can also be written on matrix form as

$$\begin{pmatrix} \alpha_1 & 0 & 0 & \alpha_2 \\ 0 & \alpha_1 & -\alpha_2 & 0 \\ 0 & -\alpha_2 & \alpha_3 & 0 \\ \alpha_1 & 0 & 0 & \alpha_3 \end{pmatrix} \begin{pmatrix} F_x \\ F_y \\ M_x \\ M_y \end{pmatrix} = \begin{pmatrix} u \\ v \\ \theta \\ \psi \end{pmatrix}, \quad (\text{A.7})$$

where $[\alpha]$ is the flexibility matrix. The stiffness matrix $[K]$ is determined by inverting the flexibility matrix $[\alpha]$.

$$[K] = \begin{pmatrix} k_1 & 0 & 0 & k_2 \\ 0 & k_1 & -k_2 & 0 \\ 0 & -k_2 & k_3 & 0 \\ k_2 & 0 & 0 & k_3 \end{pmatrix} \quad (\text{A.8})$$

References

[A.1] Teknisk Ståbi, Nyt teknisk forlag. {118}

Appendix B

B.1 Stationary vs. Rotating Reference Frame

Rotating systems can be analyzed in a stationary- or a rotating reference frame. A stationary reference frame should be used if a rotating structure (rotor) is modeled along with a stationary support structure. Examples of such an application include a wind turbine engine rotor-stator assembly where the rotor spins inside a specially designed housing. Consequently, a rotating reference frame should be where the structure has no stationary parts and the entire structure is rotating. The differences between a stationary- and a rotating reference frame are given in Table B-1, [B.1].

Stationary reference frame	Rotating reference frame
- Structure must be axis axisymmetric about the spin axis.	- Structure need not be axisymmetric about the spin axis.
- Rotating structure can be part of a stationary structure in an analysis. The stationary structure and supports (such as bearings) need not be axisymmetric.	- Rotating structure must be the only part of an analysis model.
- It is possible to create Ω - ω diagrams for computing critical speeds.	- It is <u>not</u> possible to create Ω - ω diagrams for computing critical speeds.
- Supports more than one rotating structure spinning at different rotational speeds about different axes of rotation	- Supports only a single rotating structure.
- Supported elements: BEAM4, PIPE16, MASS21, SOLID45, SOLID95, SOLID185, SOLID186, SOLID187, BEAM188, and BEAM189.	- Supported elements: MASS21, SHELL181, PLANE182, PLANE183, SOLID185, SOLID186, SOLID187, BEAM188, BEAM189, SOLSH190, and SHELL281.

Table B-1: Reference frame considerations.

The stationary reference is used in this thesis work because it gives the possibilities to analyze how machinery vibrations, including gyroscopic effects, affect a stationary structure.

References

[B.1] http://www.kxcad.net/ansys/ANSYS/ansyshelp/Hlp_G_ADVCHOOSE.html

Appendix C

C.1 Natural Frequencies for the Simple Rotor Configuration

The aim of this appendix is to derive the natural frequencies of a simple rotor system. The following Appendix is based on [C.1]. The equation of motions for the complete system is given below

$$\begin{pmatrix} m & 0 & 0 & 0 \\ 0 & m & 0 & 0 \\ 0 & 0 & I_d & 0 \\ 0 & 0 & 0 & I_p \end{pmatrix} \begin{pmatrix} \ddot{x} \\ \ddot{y} \\ \ddot{\theta} \\ \ddot{\psi} \end{pmatrix} + \begin{pmatrix} 0 & 0 & 0 & 0 \\ 0 & 0 & 0 & 0 \\ 0 & 0 & 0 & I_p \\ 0 & 0 & -I_p & 0 \end{pmatrix} \begin{pmatrix} \dot{x} \\ \dot{y} \\ \dot{\theta} \\ \dot{\psi} \end{pmatrix} + \begin{pmatrix} k_1 & 0 & 0 & k_2 \\ 0 & k_1 & -k_2 & 0 \\ 0 & -k_2 & k_3 & 0 \\ k_2 & 0 & 0 & k_3 \end{pmatrix} \begin{pmatrix} x \\ y \\ \theta \\ \psi \end{pmatrix} = m\epsilon\Omega^2 \begin{pmatrix} \cos(\Omega t) \\ \sin(\Omega t) \\ 0 \\ 0 \end{pmatrix}. \quad (C.1)$$

The natural frequencies of the system is obtained by setting the right hand side of (C.1) to zero. The elastic coupling k_2 vanish because the disk is centrally mounted on the shaft and the equation of motions yields

$$m\ddot{x} + k_1x = 0 \quad (C.2)$$

$$m\ddot{y} + k_1y = 0 \quad (C.3)$$

$$I_d\ddot{\theta} + I_p\Omega\dot{\psi} + k_3\theta = 0 \quad (C.4)$$

$$I_d\ddot{\psi} - I_p\Omega\dot{\theta} + k_3\psi = 0 \quad (C.5)$$

The first two equations are uncoupled and can be solved independently. The general solution of equation (C.2) and (C.3) can be found by applying a general solution technique to solve 2nd order linear differential equation with constant coefficients can be written as

$$x(t) = \sum_{n=1}^N X_n \exp(S_n t) \quad (C.6)$$

where X_n and s_n are complex constants The same principle is valid for the response to $y(t)$.

Thus, $\ddot{x} = s_n^2 X_n \exp(s_n t)$, substituting this relationship into equation (C.2), one obtains

$$m \sum_{n=1}^2 X_n s_n^2 \exp(s_n t) + k \sum_{n=1}^2 X_n \exp(s_n t) = 0, \quad (C.7)$$

rewritten as

$$\sum_{n=1}^2 X_n (ms_n^2 + k) \exp(s_n t) = 0 \quad (C.8)$$

The nontrivial solution of equation (C.8) $X_n \neq 0$ can only be satisfied if the following characteristic equation is satisfied; $ms_n^2 + k = 0$. The characteristic exponents s_n , are the roots of this equation.

$$s_1 = s_3 = i \sqrt{\frac{k_1}{m}}, \quad s_2 = s_4 = -i \sqrt{\frac{k_1}{m}}, \quad (\text{C.9})$$

where $i = \sqrt{-1}$. The roots given by (C.9) are complex conjugate pairs and the systems natural whirling frequencies is determined by

$$\omega_1 = \omega_2 = \sqrt{\frac{k_1}{m}} \quad (\text{C.10})$$

The second pair of equations is coupled and again the solution is assumed on the form.

$$\theta(t) = \sum_{n=1}^4 \theta_n \exp(S_n t) \quad \psi(t) = \sum_{n=1}^4 \psi_n \exp(S_n t) \quad (\text{C.11})$$

Substituting this relationship into (C.4) and (C.5), one obtains

$$\begin{aligned} I_d \sum_{n=1}^4 \theta_n s_n^2 \exp(s_n t) + I_p \sum_{n=1}^4 s_n \psi_n \exp(s_n t) + k_3 \sum_{n=1}^4 \theta_n \exp(S_n t) \\ = 0, \\ I_d \sum_{n=1}^4 \psi_n s_n^2 \exp(s_n t) - I_p \sum_{n=1}^4 s_n \theta_n \exp(s_n t) + k_3 \sum_{n=1}^4 \psi_n \exp(S_n t) \\ = 0, \end{aligned} \quad (\text{C.12})$$

rewritten as

$$\sum_{n=1}^4 \{(I_d s_n^2 + k_3) \theta_n + I_p \Omega s_n \psi_n\} \exp(s_n t) = 0, \quad (\text{C.13})$$

$$\sum_{n=1}^4 \{-I_p \Omega s_n \theta_n + (I_d s_n^2 + k_3) \psi_n\} \exp(s_n t) = 0. \quad (\text{C.14})$$

The expression in the brackets are satisfied at all times if θ_n, ψ_n and $\exp(s_n t)$ is eliminated. This leads to

$$(I_d s_n^2 + k_3)^2 + (I_p \Omega s_n)^2 = 0 \quad (\text{C.15})$$

Moving the last term to the right side of the equation and taking the square root gives

$$I_d s_n^2 + k_3 = \pm i I_p \Omega s_n \quad \text{or} \quad I_d s_n^2 \mp i I_p \Omega s_n + k_3 = 0 \quad (\text{C.16})$$

The four roots $s_5 - s_8$ to this second order polynomial are complex conjugate pairs. The result is given below

$$s_{5,7} = i \left\{ \pm \frac{I_p \Omega}{2I_d} + \sqrt{\left(\frac{I_p \Omega}{2I_d} \right)^2 + \frac{k_3}{I_d}} \right\}, \quad s_{6,8} = -s_{5,7} \quad (\text{C.17})$$

The speed of the rotation have an influence on the root and consequently also on the natural frequency. The roots s_5 and s_7 , and the complex conjugate pair s_6 and s_8 , are equal when the rotation speed is zero.

The natural whirling frequencies of the system is determined from $s_5 = i\omega_3$, and $s_7 = i\omega_4$.

$$\omega_3 = -\frac{I_p \Omega}{2I_d} + \sqrt{\left(\frac{I_p \Omega}{2I_d} \right)^2 + \frac{k_3}{I_d}}, \quad \omega_4 = \frac{I_p \Omega}{2I_d} + \sqrt{\left(\frac{I_p \Omega}{2I_d} \right)^2 + \frac{k_3}{I_d}}, \quad (\text{C.18})$$

It can then be seen that the natural frequency ω_3 is decreasing with increasing rotational speed, and ω_4 is increasing with increasing with increasing rotational speed. This behavior is due to the influence of the gyroscopic effect which is caused by the wobbling of the disk. Equation (C.18) can be used to create a Ω - ω diagram.

References:

[C.1] Michael I. Friswell et al. Dynamics of rotating machines, 1 edition 2010.

Appendix D

D.1 Modeling of Bearings

Bearings are designed to support and transfer pure radial load, pure axial loads or a combination. Bearings are not infinite stiff and the friction and lubrication of them introduce damping. Bearings can be visualized as springs, and often springs have stiffness and damping that varies with speed and direction. A typical roller bearing is illustrated in Figure D.1.

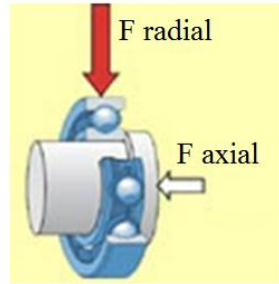


Figure D.1 Typically Roller Bearing and forces acting on it, [D.1].

Bearings are modeled in Ansys with one of the following element types, listed in Table D.1.

	Description	Stiffness and Damping cross terms	Nonlinear stiffness and damping characteristics	Geometry
COMBIN14 Spring/damper per Element	Uniaxial spring/damper	No	No	
COMBI214 Spring/damper per Element	2-D spring/damper	Unsymmetric	Stiffness and damping characteristics can be given as a function of the rotational velocity	

Table D-1: Spring/damper elements in Ansys [D.2], [D.3].

COMBIN14 is a spring/damper with longitudinal or torsional capability in 1-D, 2-D, or 3-D applications. The longitudinal spring-damper option is a uniaxial tension-compression element. The spring-damper element has no mass. Masses can be added by using MASS21 elements. The spring and damping coefficient is constant, i.e. the parameters cannot vary with spin velocity.

COMBI214 is a spring/damper with longitudinal as cross-coupling capability in 2-D applications. The spring-damper element has no mass. The spring stiffness and damping can vary with spin velocity.

References

[D.1] <http://www.skf.com/skf/support/html/dictionary/dictionary.jsp?dictPage=r&lang=en>

[D.2] http://www.kxcad.net/ansys/ANSYS/ansyshelp/Hlp_E_COMBIN14.html

[D.3] http://www.kxcad.net/ansys/ANSYS/ansyshelp/Hlp_E_COMBI214.html

Appendix E

E.1 Analysis of the Support Springs

In this appendix we analyze how the spring stiffness of the springs connected to the support structure affect the dynamic response of the tower. The spring elements are illustrated in Figure E.1. The spring stiffness is analyzed in the interval $k = 10^4 - 10^{12} \text{ kN/m}$.

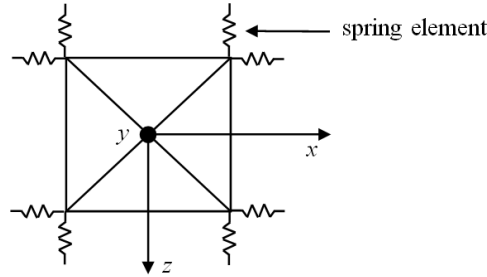


Figure E.1 Illustration of the spring elements attached to each corner of the support structure.

The dynamic response, including the bending moment M_z , the gyroscopic torque T and the bending moment M_x , see Figure E.2, is analyzed for a varying spring stiffness. The spring stiffness is analyzed in the interval $k = 10^4 - 10^{12} \text{ N/m}$.

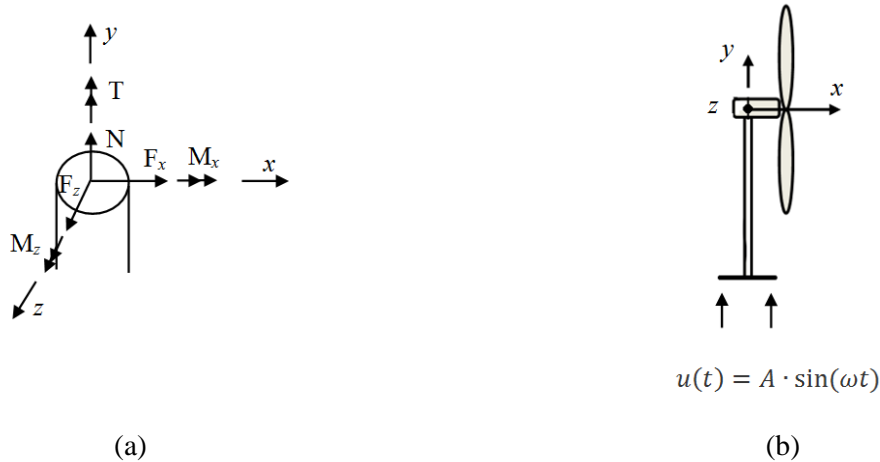


Figure E.2 (a) section forces in the BEAM188 element. (b) illustration of the wind turbine.

The results are given in Figure E.3, Figure E.4 and Figure E.5

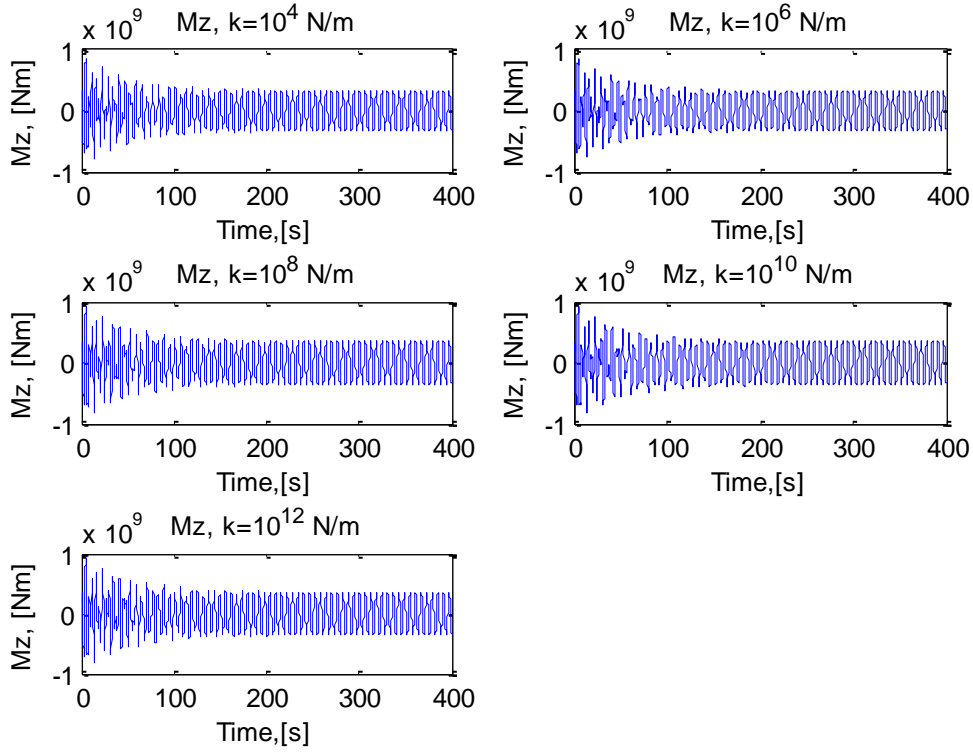


Figure E.3 Bending moment M_z for spring stiffness $k = 10^4 - 10^{12}$ N/m.

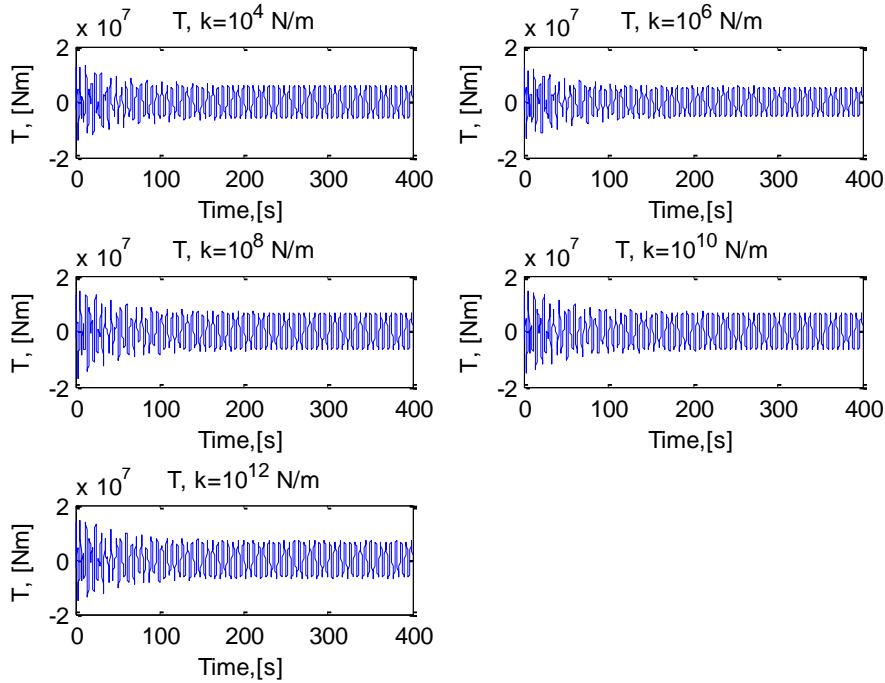


Figure E.4 Gyroscopic torque T for spring stiffness $k = 10^4 - 10^{12}$ N/m.

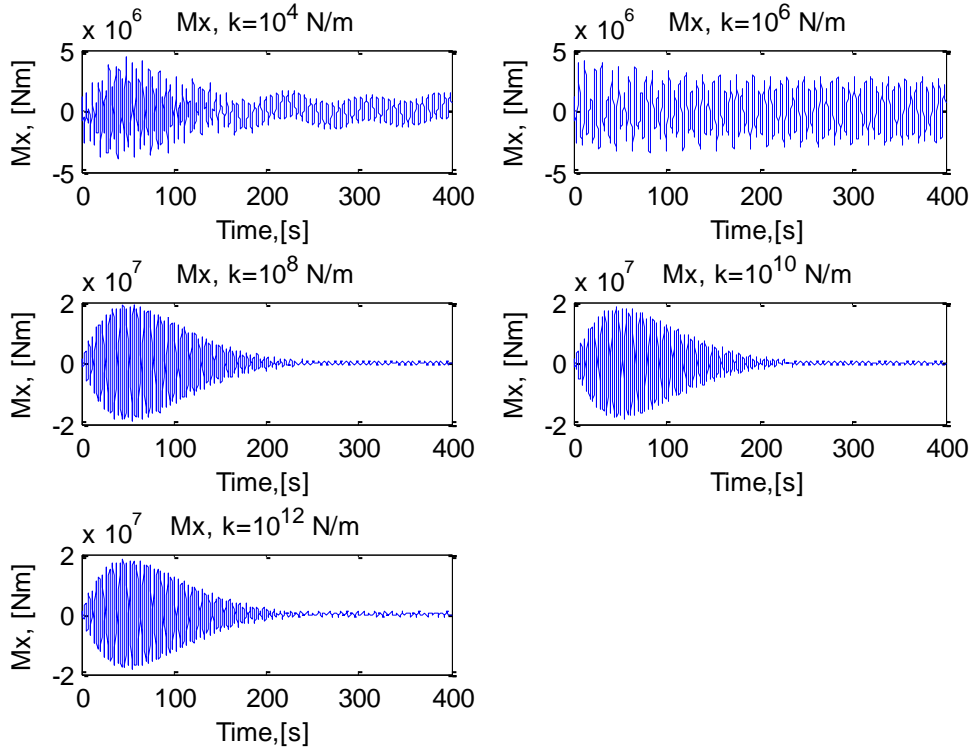


Figure E.5 Bending moment M_x for spring stiffness $k = 10^4 - 10^{12} \text{ N/m}$.

Figure E.3 and Figure E.4 shows that the the bending moment M_z and the gyroscopic T are not affected by the spring stiffness. Figure E.5 shows that the bending moment M_x is affected by the spring stiffness. As a result, we obtain a value of M_x which is increased with a factor 2 for $k = 10^6 \text{ N/m}$ compared to $k = 10^{12} \text{ N/m}$. The spring stiffness $k = 10^6 \text{ N/m}$ is used in all analysis.

Lowering the spring stiffness result in an increased rotation of the support structure which result in an increased transverse shear force F_z that increase the bending moment M_x . This explains why the bending moment M_x is increased when the spring stiffness is decreased.

Appendix F

F.1 Solving the Equation of Motion for a Simple System

A harmonic motion is principally applied in the same manner as a harmonic load in Ansys. A simple example, shown in Figure F.1, is applied a harmonic force in the top and harmonic displacement in the bottom. This example is analyzed analytically and in Ansys and the results are compared. This is done to ensure that we apply the harmonic force and displacement correct in Ansys.

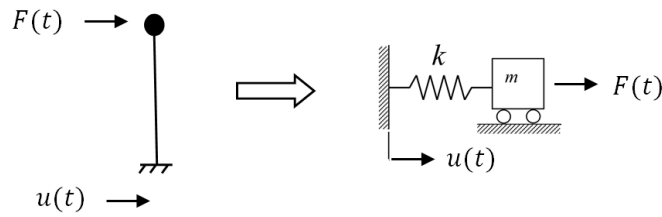


Figure F.1 Spring mass system.

The equation of motion for the mass spring system is

$$m\ddot{x} + Kx - Ku_0\sin(\omega t) = F_0\cos(\omega t). \quad (\text{F.1})$$

Substituting $k=100$, $m=400$, $\omega=1$, $u_0=0.1$, $F_0=1$ and setting the initial conditions $x(0) = 0$ and $\dot{x}(0) = 0$, one obtains the solution for the displacement $x(t)$ of the mass. The result is obtained in Maple, see section F.2. The same system is modeled in Ansys and transient analysis is performed. The results of the analytical solution (blue) and Ansys (red) are shown in Figure F.2.

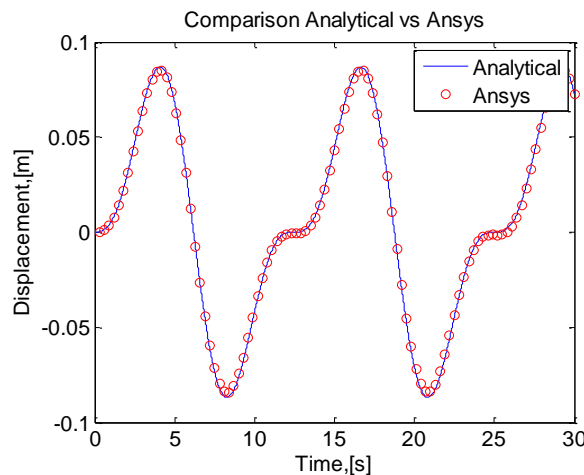


Figure F.2 Time response of the displacement of the mass.

The analytical result is similar to the Ansys result, i.e. it must be concluded that we are able to apply the harmonic displacement- and force correct in Ansys.

F.2 Solving the Equation of Motion in Maple

The equation of motion for the mass spring system is solved in Maple. The Maple script is given below:

```
> restart;
> EM := m*(diff(x(t), t, t)) = -K*x(t)+K*u[0]*sin(omega*t)
+F0*cos(omega*t);
```

$$EM := m \left(\frac{d^2}{dt^2} x(t) \right) = -K x(t) + K u_0 \sin(\omega t) + F_0 \cos(\omega t)$$

Initial Conditions

```
> Init1:=x(0)=x0;
```

$$Init1 := x(0) = x_0$$

```
> Init2:=D(x)(0)=v0;
```

$$Init2 := D(x)(0) = v_0$$

The solution

```
> dsolve({EM, Init1, Init2}, x(t));
```

$$x(t) = \frac{\sin\left(\frac{\sqrt{K} t}{\sqrt{m}}\right) \sqrt{m} \left(v_0 K - v_0 m \omega^2 - K u_0 \omega\right)}{\sqrt{K} (K - \omega^2 m)} - \frac{\cos\left(\frac{\sqrt{K} t}{\sqrt{m}}\right) (-x_0 K + x_0 \omega^2 m + F_0)}{K - \omega^2 m} + \frac{K u_0 \sin(\omega t) + F_0 \cos(\omega t)}{K - \omega^2 m}$$

```
> x(t) := rhs(%);
```

Substitution of numerical values into the solution.

```
> x_plot:=subs([v0=0, x0=0, K=100, m=400, F0=1, omega=1, u[0]=0.1], x(t));
```

$$x_plot := 0.0003333333333 \sin\left(\frac{1}{400} \sqrt{400} \sqrt{100} t\right) \sqrt{400} \sqrt{100} + \frac{1}{300} \cos\left(\frac{1}{400} \sqrt{400} \sqrt{100} t\right) - 0.03333333333 \sin(t) - \frac{1}{300} \cos(t)$$

Plotting the mass displacement as function of time

```
> plot(x_plot, t=0..30);
```

Appendix G – Results Chapter 7

G.1 Displacement in the x-Direction for Model 1 and Model 2

The displacement in the x-direction is similar for model 1 model 2 in node 10 (and all other nodes). This is illustrated in Figure G.1.

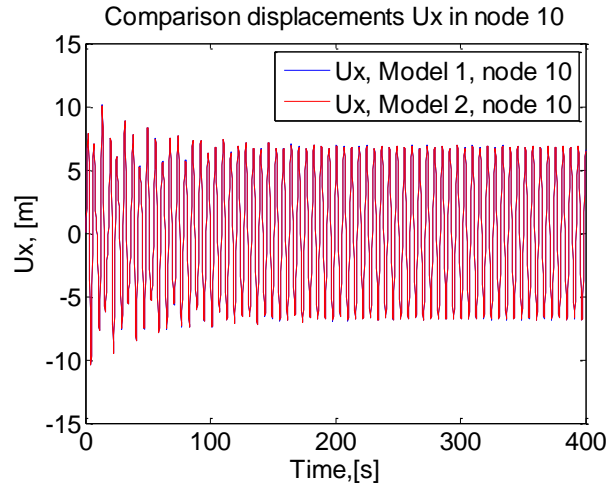


Figure G.1 Comparison of displacements in the x-direction for model 1 and model 2, in node 10.

G.2 Rotations about the z-axis for Model 1 and Model 2

The rotation about the z-axis is about 1 percent smaller for model 2 than model 1. This is illustrated in Figure G.2

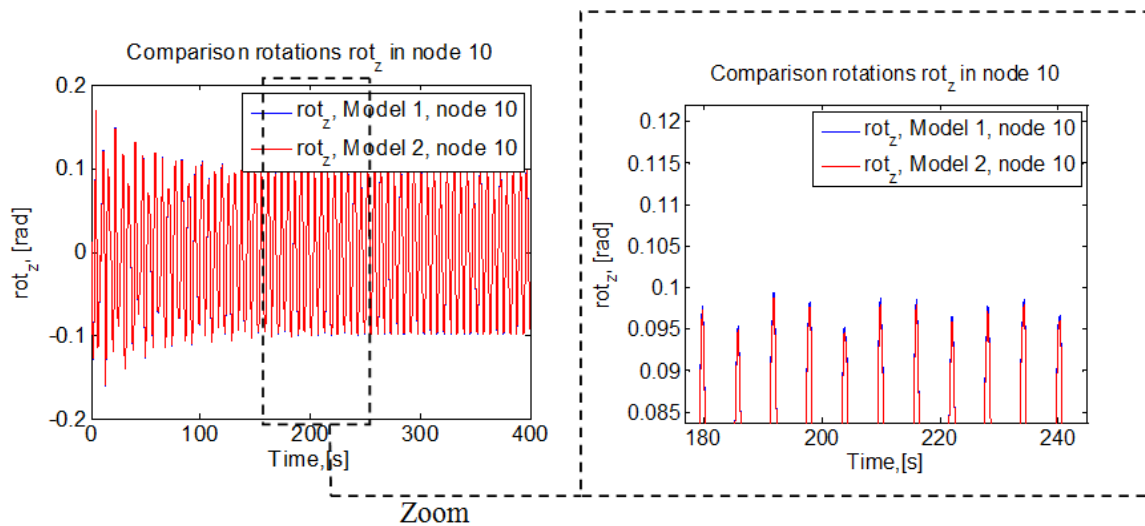


Figure G.2 Comparison of displacements in the x-direction for model 1 and model 2, in node 10.

G.3 Rotation about the y-axis Model 2

The rotation about the y-axis is shown in Figure G.3.

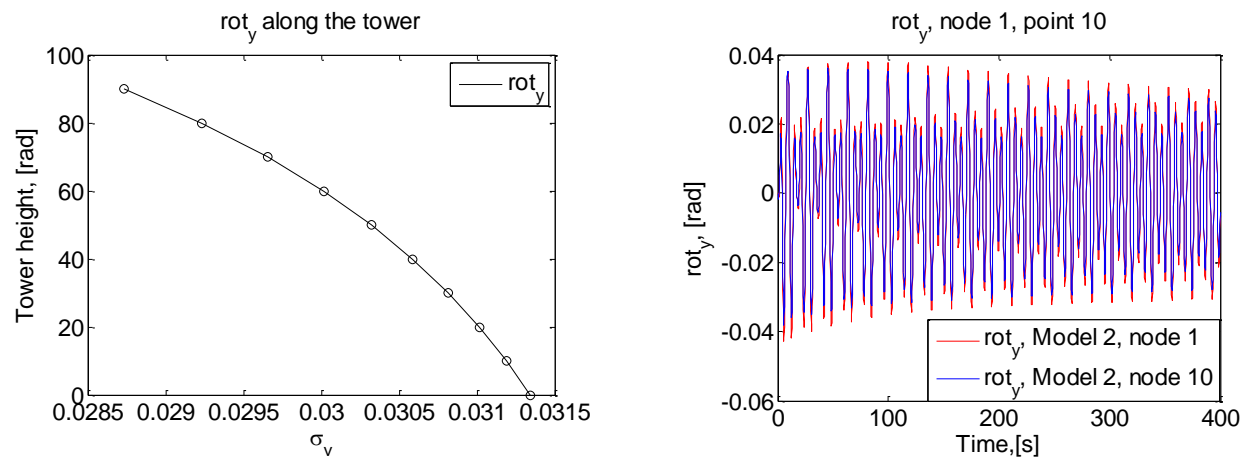


Figure G.3 rotation about the y-axis.

Appendix H

The purpose of this appendix is to explain the steps required to perform a harmonic analysis in Ansys. This is done for the rotor configuration presented in chapter 3. A harmonic analysis is performed numerically and analytically, and the results are compared. Harmonic analysis is used to determine the frequency response of a structure to harmonically time-varying loads, such as unbalance forces.

H.1 Unbalance load

An unbalance force rotates synchronously with the structure. The unbalance force is a function of the unbalance mass m , the distance ε from the center of rotation and the rotational velocity of the shaft Ω to the power of two; this is illustrated in Figure H.1 (a). The load is purely radial, as shown in Figure H.1 (b), because the mass is spinning with a uniform velocity.

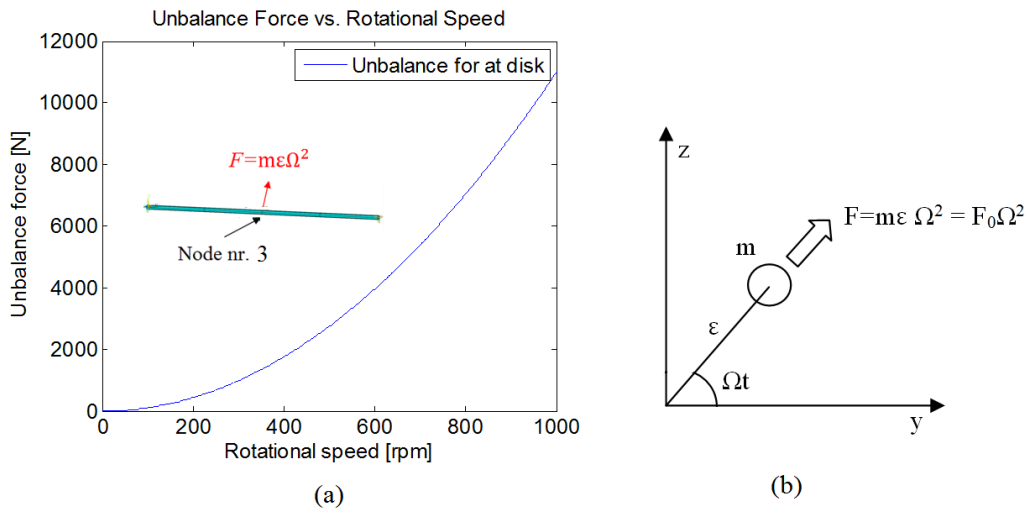


Figure H.1 (a) unbalance force vs. rotation speed. The unbalance mass is 110 kg and the eccentricity is 0.0001 m. (b). The load is purely radial because the mass is spinning with a uniform velocity.

H.2 Harmonic Analysis in Ansys

There are basically three methods for conducting a harmonic analysis (ANTYPE, HARMIC). These 3 methods are the full, reduced and modal Superposition methods [H.1]. The Full method is used in this thesis work.

Unbalance forces are applied via the 'SYNCHRO, RATIO, Cname' command. 'RATIO' defines the ratio between the unbalance force and the rotational velocity of the rotating shaft. This value is 1 for a synchronous force. 'Cname' is the name of the rotating component; defined with the 'CM' command. The harmonic analysis is conducted in a frequency interval between 0-16.66 HZ (0-1000 rpm.) via the 'HARFRQ' command. The rotational velocity Ω of the shaft is applied along the direction cosines of the rotation axis with the 'cmomega' command. Conse-

quently, the load has to be applied in a complex plane. The load on the y-axis is defined as the positive real value and the load on z-axis is defined as a negative imaginary value. The loads are defined as follows

$$F_y = F_0 \cos(\Omega t) = F_0 e^{i\Omega t}, \quad (\text{H.1})$$

$$\begin{aligned} F_z &= F_0 \sin(\Omega t) = F_0 \cos\left(\Omega t - \frac{\pi}{2}\right) \\ &= -iF_0 e^{i\Omega t}, \end{aligned} \quad (\text{H.2})$$

where F_0 is the mass m times the eccentricity ε . The remaining part of the force, the rotational velocity Ω to the power of two, is automatically included in Ansys. The loads F_y and F_z are applied to the nodes with the 'F' command. The batch file below shows how to define and apply the load. The LGW file can be found on the attached CD [LGW_13].

Code:

```
! ** Unbalance forces (eccentric mass * radius)
mass = 110                      ! The unbalance mass 0.1 g
e = 0.0001                     ! Eccentricity (distance from the center of rotation)
f0 = mass*e                     ! Unbalance force
f,3,fy,f0                       ! Load applied in node 5. Real part
f,3,fz,-f0                      ! Load applied in node 5. Complex part
```

The next step is to set up the solution procedure for the harmonic analysis. This is illustrated in the batch file below.

Code:

```
/SOLU
antype,harmic                  ! The analysis type is harmonic
SYNCHRO,,shaft                 ! Specifies that the excitation frequency is synchronous and
                                ! that the name of the rotating part is shaft
nsubst,500                     ! Number of sub steps
HARFRQ,,1000/60                ! •Frequency at end of the range
kbc,1                           ! Step loading
cmomega,shaft,100.             ! Specifies the rotational velocity
coriolis,on,,,on               ! Includes the Coriolis force in a stationary reference frame
solve                           ! Solve the system
Finish
```

The results of the harmonic analysis are presented in section 4.3.

H.3 Analytical Solution

The equation of motion for the simple rotor model is given below.

$$m\ddot{y} + k_1y + c_1\dot{y} = m\varepsilon\Omega^2\cos(\Omega t) \quad (\text{H.3})$$

$$m\ddot{z} + k_1z + c_1\dot{z} = m\varepsilon\Omega^2\sin(\Omega t) \quad (\text{H.4})$$

The steady state solution to (H.3) [H.2] is $X\cos(\omega t - \alpha)$. Here

$$|X| = \frac{\varepsilon\Omega^2}{\sqrt{((\omega_n^2 - \Omega^2)^2 + (2\Omega\xi\omega_n)^2)}}, \quad \text{and} \quad \alpha = \tan^{-1}\left(\frac{2\Omega\xi\omega_n}{\omega_n^2 - \Omega^2}\right), \quad (\text{H.5})$$

where Ω is the rotational speed of the rotor, ε is the excentricity of the unbalance, $\omega_n = \sqrt{\frac{k_1}{m}}$ and $\xi = c_1/(2m\omega_n)$. Similarly, equation (H.4) has the steady-state solution of the form $X\sin(\omega t - \alpha)$.

The amplitude of the out-of-balance force is proportional to ε , and Ω^2 , and tends to zero at low rotational speed. The unbalance force is of minor influence if $\Omega \gg \omega_n$. When the damping ratio is small and Ω is close to ω_n , the amplitude of the orbit becomes large and can cause major damage, in terms of operational problems, and ultimately in form of fatigue damage. This condition is called resonant and occurs when an excitation frequency (shaft speed) coincides with a natural frequency of the system.

H.4 Comparison – Numerical and Analytical Solution

The result from the harmonic analysis, based on the analytical solution and Ansys, is shown in Figure H.2. The Matlab plotting routine [Matlab_7] is attached on the CD.

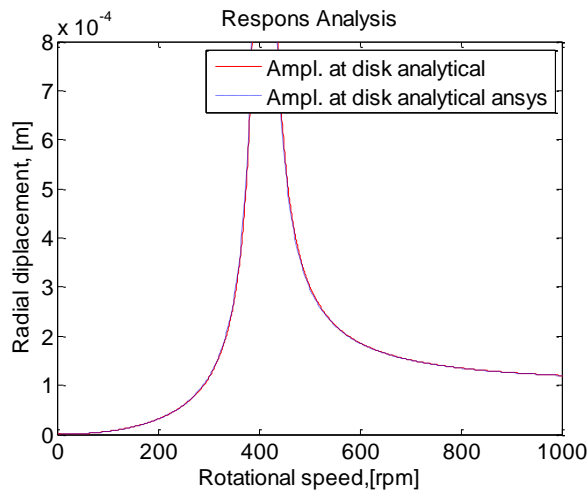


Figure H.2 Response analysis for the analytical- and numerical solution.

The result from Ansys and the analytical solution is similar.

It can be seen from Figure H.2 that the amplitude tends to infinity when the rotor passes the critical speed (400 rpm). There are in principle three approaches to the problem of minimizing the amplitudes of the whirl:

1. Balance the rotor, i.e. minimize the eccentricity.
2. Change the operating speed (away from the critical speed).
3. Add damping to the rotor/bearing system

Balancing the rotor is the most direct approach, because it removes the source of the vibration. Changing the operating speed implies a change in the rotor stiffness, the support stiffness, or a combination of these. Approach 3 is only relevant if the critical speed must be traversed slowly or repeatedly, or if an operating speed close to the critical speed cannot be avoided. Damping will not have effect if the operational speed is far away from the critical speed.

References

[H.1] http://www.kxcad.net/ansys/ANSYS/workbench/ds_harmonic_analysis_type.html

[H.2] Daniel J. Inman. Engineering Vibrations. Third Edition. { 139 }

